DRAFT
COMPLETION REPORT
INTERMEDIATE WELL I-6
LOS ALAMOS NATIONAL LABORATORY
LOS ALAMOS, NEW MEXICO
PROJECT NO. 49436

Prepared for:

The US Department of Energy and the
National Nuclear Security Administration through the
US Army Corps of Engineers
Sacramento District

Prepared by:

KLEINFELDER

8300 Jefferson NE, Suite B
Albuquerque, New Mexico 87113

TABLE OF CONTENTS

TABLE OF CONTENTS (continued)

Figures

Tables

Appendixes

LIST OF ACRONYMS AND ABBREVIATIONS

bgs	below ground surface
DOE	US Department of Energy
DTH	down-the-hole
DTW	depth to water
ft	foot/feet
gal.	gallon
gpd	gallons per day
in.	inch
Kleinfelder	Kleinfelder, Inc.
LANL	Los Alamos National Laboratory
NMED	New Mexico Environment Department
OD	outside diameter
psi	pounds per square inch
SMO	Sample Management Office
TD	total depth
WDC	WDC Exploration & Wells

ABSTRACT

Intermediate well I-6 was installed as part of the Risk Reduction and Environmental Stewardship-Remediation Services project at Los Alamos National Laboratory (LANL) in accordance with the "Mortandad Canyon Groundwater Work Plan, Revision 1" (LANL, 2004) and the Final Drilling Plan for Intermediate Wells, Mortandad Canyon (Kleinfelder, 2004). The US Department of Energy, with technical assistance from LANL, contracted and directed the installation of this well.

Data from I-6 will be used in conjunction with data from other wells in Mortandad Canyon to improve the conceptual model of the geology, hydrogeology, and hydrochemistry of the area to provide data for numerical models that address contaminant migration in the vadose (unsaturated) zone. This information will be used to facilitate decision-making with regard to regulatory compliance, risk assessment, and remediation.

The majority of the fieldwork was completed from November 3, 2004, through January 3, 2005, during which a separate corehole and borehole were drilled. The core hole was drilled to assess contaminant profiles in the first 500 feet (ft) of the subsurface. The actual core collection interval was from 4 to 498 ft below ground surface (bgs). Video and geophysical logs were run before the corehole was backfilled with bentonite and abandoned. The borehole was drilled to a depth of 720 ft bgs using air-rotary drilling methods and was completed as a monitoring well. The lithology encountered during borehole drilling included (in descending order): alluvium, Tshirege member of the Bandelier tuff, Cerro Toledo interval, Otowi member of the Bandelier tuff, Guaje pumice bed, Puye formation, and Cerros del Rio basalt.

I-6 was completed with a single-screened interval from 686 to 708 ft bgs, near the base of the Cerros del Rio basalt. The total depth of the well was 713 ft bgs. On January 21, 2005, the depth to water after well installation was 665.80 ft bgs.

1.0 INTRODUCTION

This completion report summarizes the site preparation, drilling, sampling and related activities for intermediate well I-6. Kleinfelder, Inc. (Kleinfelder), under contract to the US Army Corps of Engineers, was responsible for drilling, installing, testing, and sampling activities. The US Department of Energy (DOE) and the Los Alamos National Laboratory (LANL) funded and directed this work.

Intermediate well I-6, located within Mortandad Canyon (Figure 1.0-1), was installed to assess the lateral extent of a contaminated intermediate perched zone encountered in nearby characterization well R-15. Data quality objectives for this and other intermediate wells are provided in the "Mortandad Canyon Groundwater Work Plan" (LANL, 2004) and the "Final Drilling Plan for Intermediate Wells" (Kleinfelder, 2004). Water quality, geochemical data, aquifer characteristics, and geologic information obtained will augment the conceptual model and knowledge of contaminant distribution in the intermediate perched zone in Mortandad Canyon system.

The objectives of the coring and drilling activities were to collect core and cuttings of encountered geologic formations, collect groundwater samples from the perched intermediate aquifer, and install a single-screened monitoring well near the base of the Cerros del Rio basalt. A separate corehole for collecting core and borehole for well installation were drilled. The core hole was drilled to assess contaminant profiles in the first 500 feet (ft) of the subsurface. The projected total depth (TD) of the borehole was 760 ft below ground surface (bgs) (LANL, 2004). The actual TD of the I-6 borehole was 720 ft bgs.

The information presented in this report was compiled from field reports and activity summaries generated by Kleinfelder, LANL, and subcontractor personnel. Original records, including field reports, field logs and survey records, are on file in Kleinfelder's Albuquerque office and LANL's Records Processing Facility. Detailed analysis and interpretation of geologic, geochemical, and aquifer data will be included in separate technical documents to be prepared by LANL.

2.0 DRILLING ACTIVITIES

From October 21 through November 3, 2004, the I-6 corehole was cored to characterize vertical contaminant profiles in the vadose zone.

A separate borehole was advanced to 720 ft bgs using air-rotary drilling methods from January 3, 2005, through January 13, 2005. A groundwater monitoring well was installed in this borehole to 713 ft bgs. Drilling activities were performed generally in one 12-hour shift per day, 7 days per week, by the drill crew and two site geologists. Depth-to-water (DTW) measurements were taken at the beginning and end of most shifts to assess for groundwater.

2.1 Coring Activities

Spectrum Exploration, Inc., performed coring operations using a Delta Base DB540 drill rig equipped with HQ_3 Coring, Geobarrel, and 115-millimeter Tubex drilling systems.

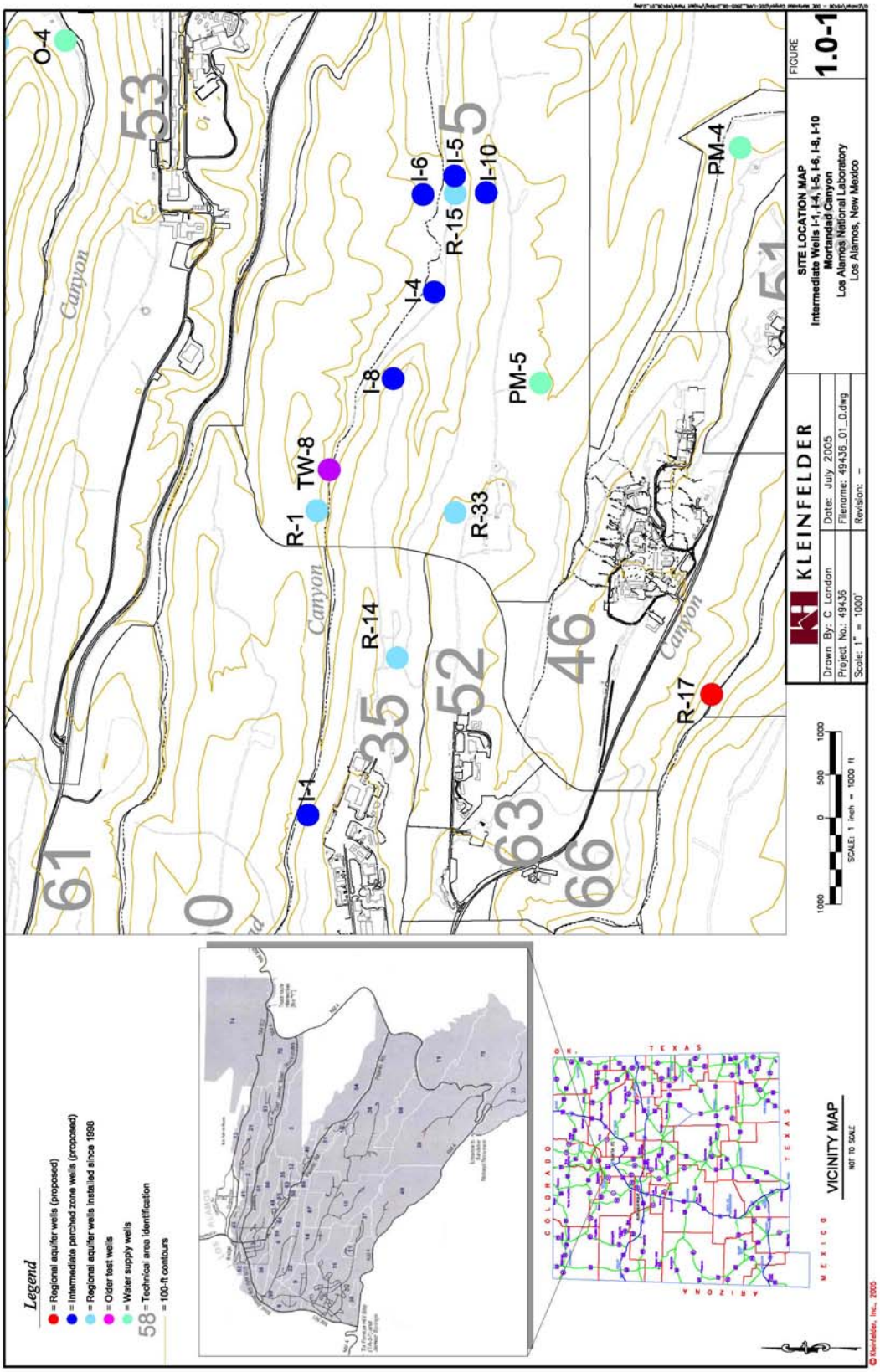
O-4
Canyon
53
I-6
I-5
I-10
R-15
5
PM-4
I-4
I-8
PM-5
TW-8
R-1
R-33
R-14
Canyon
35
52
46
61
63
66
51
I-1
R-17
Canyon
SITE LOCATION MAP
Intermediate Wells I-1, I-4, I-5, I-6, I-8, I-10
Mortandad Canyon
Los Alamos National Laboratory
Los Alamos, New Mexico
FIGURE
1.0-1
KLEINFELDER
Drawn By: C. Landon
Project No.: 49436
Scale: 1" = 1000'
Date: July 2005
Filename: 49436_01_0.dwg
Revision: -
SCALE: 1 inch = 1000 ft
1000
500
0
1000
Legend
= Regional aquifer wells (proposed)
= Intermediate perched zone wells (proposed)
= Regional aquifer wells installed since 1998
= Older test wells
= Water supply wells
58 = Technical area identification
= 100-ft contours
VICINITY MAP
NOT TO SCALE
COLORADO
TEXAS
NEW MEXICO
ARIZONA
TEXAS
© Kleinfelder, Inc., 2005

Continuous-core samples were collected from 4 to 498 ft bgs. Lithologic samples were collected during coring at depths specified in the drilling plan (Kleinfelder, 2004). Samples were submitted for moisture content determination as well as chemical analyses of anions, stable isotopes, radionuclides, metals, and tritium concentrations. Additionally, all core collected was labeled, boxed, and taken to the Field Support Facility for permanent storage. LANL Radiation Control Technicians screened the core prior to its removal from the drill site.

After reaching total depth, the corehole was backfilled with bentonite chips and abandoned.

2.2 Rotary Drilling Activities

WDC Exploration & Wells (WDC) drilled the I-6 borehole using a GEFCO 50K drill rig equipped with conventional drilling rods and drill collars, tri-cone button and mill-tooth bits, down-the-hole (DTH) hammer bits, air compressors, and support equipment. I-6 was drilled using air-rotary drilling techniques. Drilling fluids, consisting of a mixture of municipal water with QUIK-FOAM® surfactant, were used as needed to improve borehole stability and facilitate cuttings removal. An approximate tally of the total drilling fluids introduced into the borehole, as well as the total fluids recovered, is presented in Table 2.0-1.

Table 2.0-1
Introduced and Recovered Fluids

Material		**Amount (gallons)**
Introduced	QUIK-FOAM®	90
	Defoaming agent	0
	Potable water (air rotary drilling)	7,500
	EZ-MUD®	0
	Total introduced fluids[1]	7,590
Recovered	Total recovered fluids[2]	9,704

[1] Represents the fluids introduced during drilling
[2] Represents the estimated fluid volume recovered during drilling, well development and aquifer testing

On January 3, WDC completed mobilization of drilling equipment and supplies to the I-6 site. The borehole was initially drilled with a 12¼-in.-diameter tri-cone bit, which was advanced to a depth of 15 ft bgs. Concurrently, 13⅝-in. conductor casing was advanced to a depth of 15 ft bgs.

On January 4, WDC advanced the 12¼-in. diameter tri-cone bit to a depth of 285 ft bgs. The 13⅝-in. conductor casing was advanced to 60.5 ft bgs.

On January 5, WDC advanced the 12¼-in. diameter tri-cone bit to a depth of 495 ft bgs. Basalt was encountered at a depth of 495 ft bgs. WDC removed the drill string from the borehole to measure DTW and change the drill bit. Water was not present in the borehole. WDC replaced the drill bit with a 12¼-in. DTH hammer and button bit, and advanced the borehole from 495 to 515 ft bgs.

On January 6, WDC advanced the borehole from 515 ft bgs to the TD of 720 ft bgs. After removing the drill string (drill bit and drill pipe) from the borehole, the DTW was 695 ft bgs.

On the morning of January 7, the DTW was 661.65 ft bgs. A sample (CAMO-05-56789) of the borehole fluids was collected using a bailer. Borehole video and natural gamma were run into the borehole using Kleinfelder-supplied geophysical equipment.

On January 8, the DTW was measured in the borehole at 661.15 ft bgs. Borehole video and induction logs were run into the borehole using Kleinfelder-supplied geophysical equipment. At the end of the shift, the DTW was 661.15 ft bgs.

On the morning of January 9, the DTW in the borehole was 661.45 ft bgs. The bottom of the borehole was measured at 717 ft bgs. Approximately 32 gallons (gal.) of water were bailed from the borehole.

On January 10, 2005, the approved well design was delivered to the site geologists. The DTW was 661.85 ft bgs, and the TD of the borehole was 714 ft bgs. This indicated that approximately 3 ft of slough had accumulated in the bottom of the borehole. WDC installed the tremie pipe to a depth of 620 ft bgs and began installing the casing and well screen, as designed.

On January 11, 2005, WDC completed construction of the well and placement of annular fill materials to a depth of 291 ft bgs.

On January 12, 2005, WDC completed placement of annular fill materials to a depth of 90 ft bgs and began demobilization activities.

On January 13, 2005, WDC pulled the 13⅝-in. conductor casing from the borehole and filled the upper 90 ft of borehole annular space with cement slurry with 2% bentonite. Afterwards, they demobilized the drill rig and equipment from the drill site.

3.0 SAMPLING ACTIVITIES

Core, cuttings, groundwater screening samples, and waste characterization samples were collected at I-6. Sampling activities were conducted in accordance with the drilling plan (Kleinfelder, 2004).

3.1 Sampling of Core and Drill Cuttings

Core was collected from 4 to 480 ft bgs and was sampled to analyze for anions, cations, moisture content, radionuclides, and stable isotopes (Table 3.1-1). Approximately 500 to 1,000 grams of core sample were placed in appropriate sample jars and protective plastic bags for delivery to LANL's Sample Management Office (SMO). The remaining core was placed in lay-flat plastic tubing, labeled, and stored in standard LANL Environmental Restoration core boxes, which were transported to the Field Support Facility for archiving and storage.

As drilling conditions permitted, sufficient quantities of cuttings were collected at approximately 5-ft intervals from the borehole waste discharge line. Portions of the cuttings were sieved (using >#10 and >#35 mesh) and placed in chip trays along with unsieved cuttings. The cuttings were examined to determine lithologic characteristics and to prepare the lithologic log (Appendix B). An additional aliquot of the >#10 fraction of cuttings was prepared for all intervals where sufficient returns were available. The sieved fractions were placed in labeled plastic bags and

Table 3.1-1. I-6 Analyses

Location ID MO-24227 I-6

Core Samples			ANALYSES						
Sample ID	Sample interval (ft)	Date/Time	Moisture	Tritium (H3)	anions/cations	N14N15	D2H O18O16	ARS (DOT screening)	Notes
CAMO-05-56746	9-13.5	10/21/04; 16:00	x	x	x	x		x	
CAMO-05-56747	18.9-20.5	10/22/04; 08:30	x	x	x	x		x	
CAMO-05-56748	30-31.2	10/22/04; 10:00	x	x	x	x		x	
CAMO-05-56749	40-41.2	10/22/04; 10:25	x	x	x	x		x	
CAMO-05-56750	47.5-49.2	10/22/04; 11:00	x	x	x	x		x	
CAMO-05-56751	58.2-59.4	10/22/04; 12:40	x	x	x	x		x	
CAMO-05-56752	68.2-69.6	10/22/04; 13:15	x	x	x	x		x	
CAMO-05-56753	77.6-78.8	10/22/04; 13:50	x	x	x	x		x	
CAMO-05-56754	91.6-92.4	10/23/04; 11:00	x		x	x		x	poor recovery, no N isotopes
CAMO-05-56755	99.6-102.2	10/23/04; 11:30	x	x	x	x		x	
CAMO-05-56756	118-119.3	10/23/04; 14:47	x	x	x	x		x	
CAMO-05-56757	140-141.7	10/23/04; 15:30	x	x	x	x		x	
CAMO-05-56758	152.5-153	10/23/04; 15:40					x	x	
CAMO-05-56759	160.8-162.3	10/23/04; 16:15	x	x	x	x		x	
CAMO-05-56760	180.7-182.2	10/23/04; 17:00	x	x	x	x		x	
CAMO-05-56761	199-200.8	10/23/04; 17:47	x	x	x	x	x	x	
CAMO-05-56762	219.2-221.2	10/23/04; 18:33	x	x	x	x		x	
CAMO-05-56763	240.4-241.9	10/24/04; 09:29	x	x	x	x		x	
CAMO-05-56764	250.5-251.5	10/24/04; 10:00					x	x	
CAMO-05-56765	260.4-261.9	10/24/04; 10:36	x	x	x	x		x	
CAMO-05-56766	280.6-282.1	10/24/04; 11:40	x	x	x	x		x	
CAMO-05-56767	299.8-301.8	10/26/04; 09:26	x	x	x	x	x	x	
CAMO-05-56768	320.7-322.2	10/26/04; 11:30	x	x	x	x		x	
CAMO-05-56769	340.3-341.8	10/26/04; 13:47	x	x	x	x		x	
CAMO-05-56770	351.6-352.6	10/26/04; 15:04					x	x	
CAMO-05-56771	360.4-361.9	10/26/04; 16:22	x	x	x	x		x	
CAMO-05-56772	380.9-382.4	10/26/04; 19:00	x	x	x	x		x	
CAMO-05-56773	401.4-402.4	10/27/04; 10:35					x	x	
CAMO-05-56774	429.7-431.2	10/27/04; 17:00	x	x	x	x		x	
CAMO-05-56775	451.5-452.3	10/27/04; 18:52					x	x	
CAMO-05-56776	473-478.3	10/28/04; 12:30	x		x	x		x	
CAMO-05-56777	496-497.5	10/28/04; 18:09	x	x	x	x	x	x	

submitted to LANL. Remaining cuttings were sealed in Ziploc® bags, labeled, and archived in core boxes. Up to seven samples may be removed by LANL for mineralogic, petrographic, and geochemical analyses. No cuttings samples were submitted for contaminant characterization.

LANL Radiation Control Technicians screened core and cuttings prior to removal from site.

3.2 Groundwater Sampling

Alluvial groundwater was encountered during coring at approximately 57.5 ft bgs. A sample (CAMO-05-56788) was collected from the open corehole prior to setting surface casing. Another groundwater sample (CAMO-05-56789) was collected on January 7, 2004, from approximately 700 ft bgs in the open borehole. On February 27, a sample (CAMO-05-56791) was collected from I-6 after well development. All samples were submitted to SMO for anions, stable isotopes, radionuclides, and metals analyses.

3.3 Waste Characterization Sampling

Samples of drill cuttings and recovered drilling fluids were collected for waste characterization on February 9, 2005. These samples were submitted to Hall Environmental Analysis Laboratory in Albuquerque, New Mexico, for anions, polychlorinated biphenyls, volatiles, metals, radionuclides, and perchlorate, and explosives analyses.

4.0 BOREHOLE LOGGING

Kleinfelder logged with both video and geophysical equipment at I-6 prior to well installation to acquire visual observations and characterize borehole conditions and hydrostratigraphy (Table 4.0-1). Project personnel used this information to facilitate well design. The video log is attached as a DVD in Appendix A.

Table 4.0-1
Borehole Logging Conducted

Operator	Date	Cased Footage (ft bgs)	Open-Hole Interval (ft bgs)	Remarks	Tools
Kleinfelder	1/07/05	0-60.5	60.5-720	Water present at TD	Video camera
Kleinfelder	1/07/05	0-60.5	60.5-720	None	Gamma
Kleinfelder	1/08/05	0-60.5	60.5-720	None	Induction
Kleinfelder	1/08/05	0-60.5	60.5-720	Water present at TD	Video camera

4.1 Video Logging

Kleinfelder personnel ran borehole video logs on January 7 and January 8 to evaluate the borehole for evidence of water zones (Table 4.0-1). Water was present at 661.65 ft bgs.

4.2 Geophysical Logging

On January 7 and 8, Kleinfelder used a Mount Sopris MGXII geophysical console to run LANL-owned natural gamma and array induction geophysical tools to approximately 525 and 720 ft bgs, respectively (Table 4.0-1). The purpose of geophysical logging was to identify geologic and hydrogeologic units, with an emphasis on gathering moisture distribution data on water-bearing zones and obtaining lithologic/stratigraphic data. The natural gamma and array induction logs are shown in Figure 4.2-1.

5.0 HYDROGEOLOGY

LANL's Earth and Environmental Sciences 6 staff provided preliminary interpretation of geologic contacts based on cores and cuttings. Groundwater occurrence is interpreted from drilling observations, open-hole video logging, geophysical logging, and water-level measurements.

5.1 Geology

Visual examination of cores, borehole drill cuttings, open-hole video logs, and preliminary geophysical logs were used to construct a stratigraphic column (Figure 5.1-1). In descending order, the stratigraphic units encountered during drilling of the I-6 borehole are alluvium, Tshirege member of the Bandelier tuff, Cerro Toledo interval, Otowi member of the Bandelier tuff, Guaje pumice bed, Puye formation, and Cerros del Rio basalt. Appendix B contains the complete lithologic log for I-6.

5.2 Groundwater Occurrence and Characteristics

Drilling observations and borehole video logs indicate a single zone of saturation in the I-6 borehole. Water was measured in the completed well at 695 ft bgs on January 6, 2005.

6.0 WELL DESIGN AND CONSTRUCTION

Kleinfelder received well construction specifications on January 9, 2005, after approval by DOE, LANL, and New Mexico Environment Department. The well was installed between January 9 and January 13, 2005.

6.1 Well Design

The "Mortandad Canyon Groundwater Work Plan" (LANL, 2004) called for a single screened interval in the base of the Cerros del Rio basalt to monitor potential contaminants and groundwater chemistry in the intermediate perched water zone above the regional aquifer. Final placement of the screened interval from 686 to 708 ft bgs was determined by evaluating geophysical data, borehole cuttings, water level measurements, and field observations.

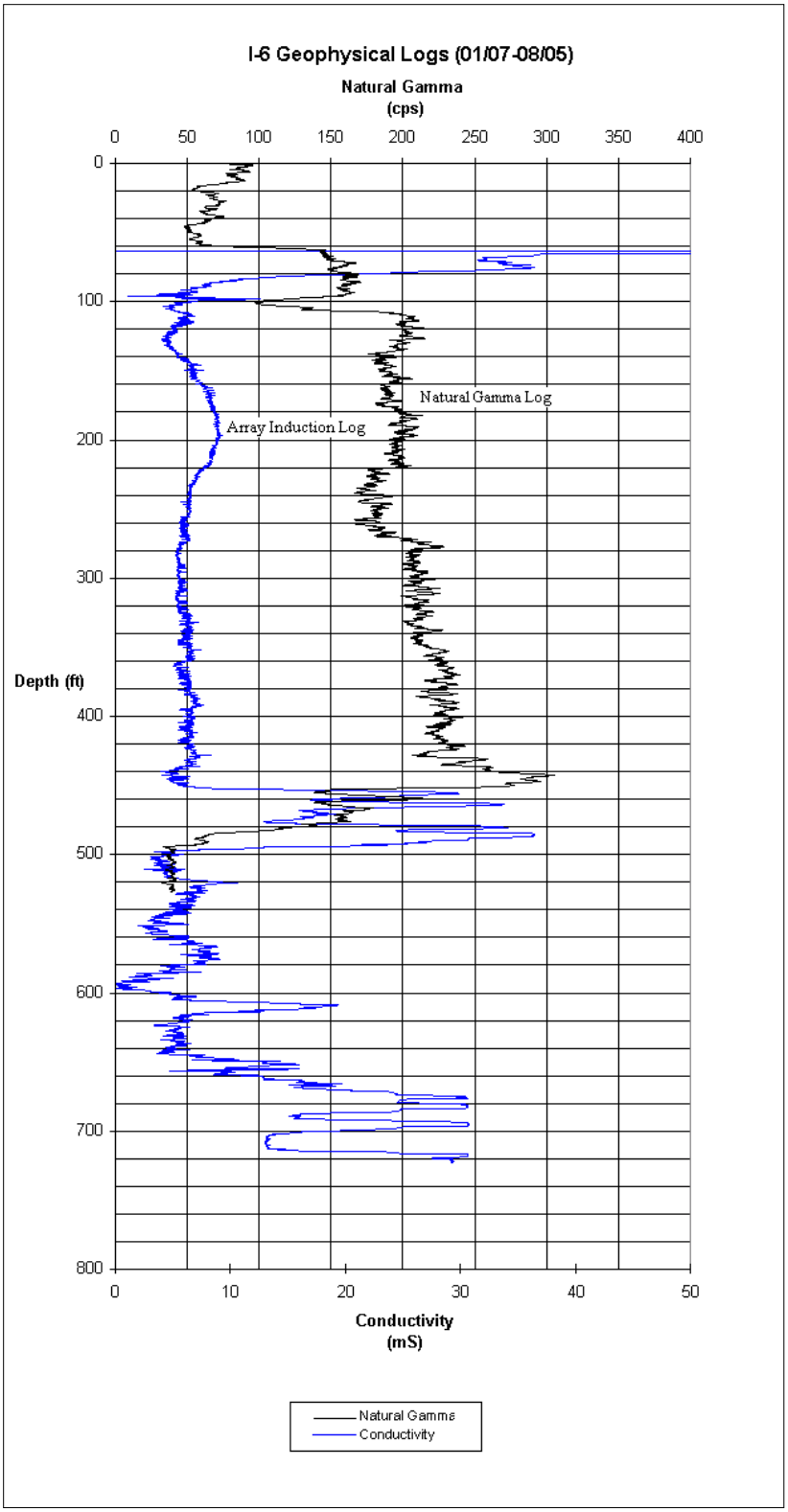

Figure 4.2-1. Natural Gamma and Induction Array Geophysical Logs

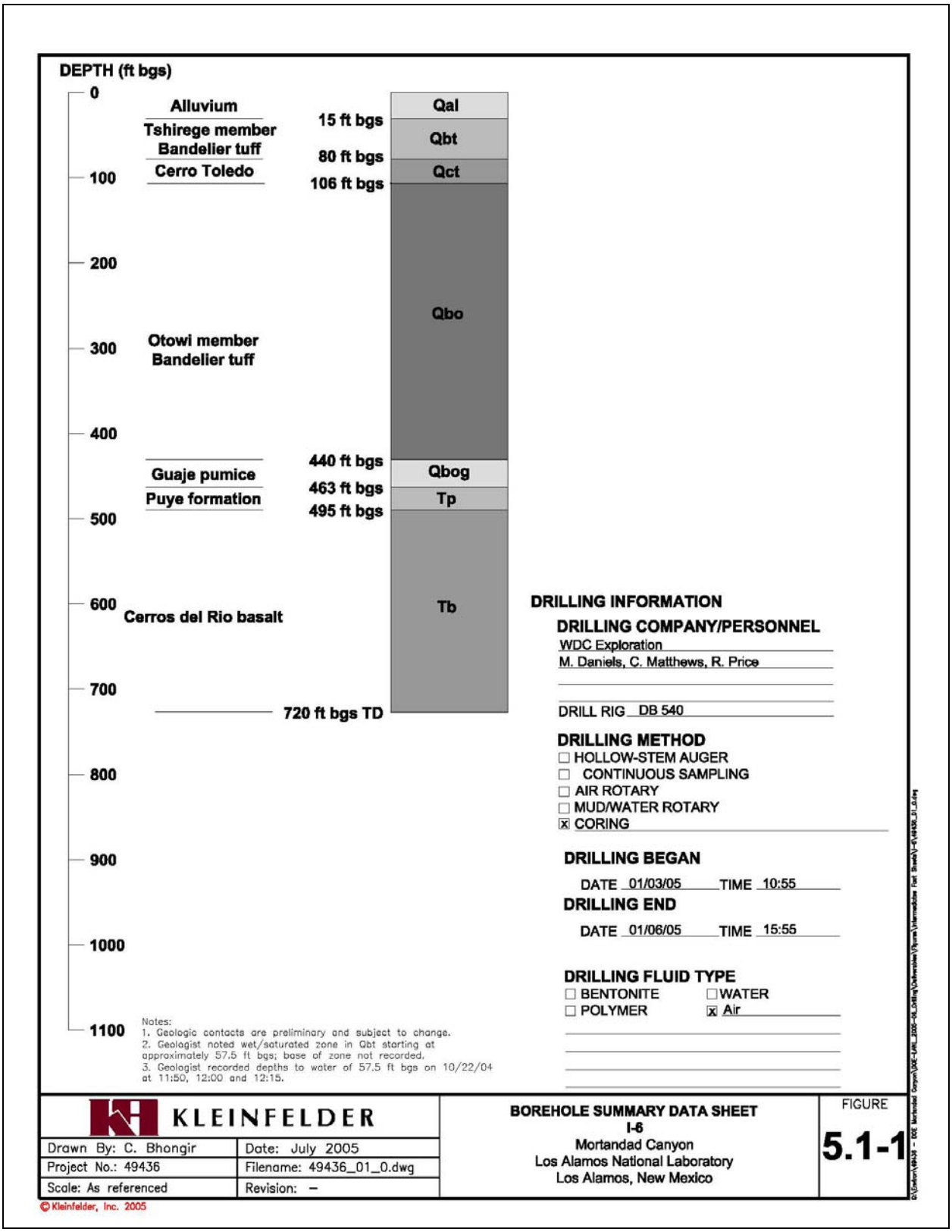

Figure 5.1-1. Borehole Summary Data Sheet for I-6

6.2 Well Construction

The casing and screen used in the construction of the I-6 well were factory-cleaned before shipment and delivery to the well site. Additionally, the stainless-steel components were decontaminated on site prior to well construction using a high-pressure hot water cleaner.

The well was constructed in accordance with LANL Environmental Restoration standard operating procedure 05.01 (LANL, 2001) using 4.5-in. inside diameter/5.0-in. outside diameter (OD), type A304, stainless-steel casing fabricated to American Society for Testing and Materials A312 standards. External couplings, also of type A304 stainless steel, were used to connect individual casing and screen joints. Two nominal 12-ft lengths of 5.27-in. OD, rod-based, 0.020-in. slot, wire-wrapped A304 stainless steel well screen (with 20 ft of screen opening) were used to construct the screened interval. A 4.94-ft-deep sump of stainless-steel casing was placed below the well screen. The screened interval was set from 686 to 708.28 ft bgs (Figure 6.2-1).

Prior to installing the tremie pipe and well casing into the borehole, approximately 100 pounds of coated bentonite pellets were placed in the bottom of the borehole to form a seal from approximately 717 to 715 ft bgs. The bottom of the borehole was measured at 714 ft bgs, indicating that 1 ft of slough had accumulated on top of the bentonite plug. A 2.5-in.-OD steel tremie pipe was used to place filter pack materials during well completion. A primary filter pack of 10/20 silica sand was placed from 714 to 669 ft bgs. After placement of the primary filter pack, WDC swabbed the screened interval to promote settling and compaction of the filter pack. A fine sand collar consisting of 20/40 silica sand was then placed above the primary filter pack from 669 to 667 ft bgs. Following placement of the fine sand collar, DTW was measured at 656.05 ft bgs. An initial seal of coated bentonite pellets was placed from 667 to 652 ft bgs. Pellets were used to delay hydration through the water column and achieve a good seal. The remaining seal consisted of bentonite chips and was placed from 652 to 90 ft bgs. The 16-in. conductor casing was removed and cement grout, consisting of 2,500 pounds per square inch (psi) concrete with 1% bentonite, was placed from 90 to 1 ft bgs. The volume of annular fill materials is summarized in Table 6.2-1

Table 6.2-1

Annular Fill Materials Used in Well Construction

Material	Volume
Surface seal: cement slurry	108 ft^3
Bentonite seal: bentonite chips	481.4 ft^3
Fine sand collar: 20/40 silica sand	1.5 ft^3
Primary filter: 10/20 silica sand	33 ft^3
Potable water	700 gallons

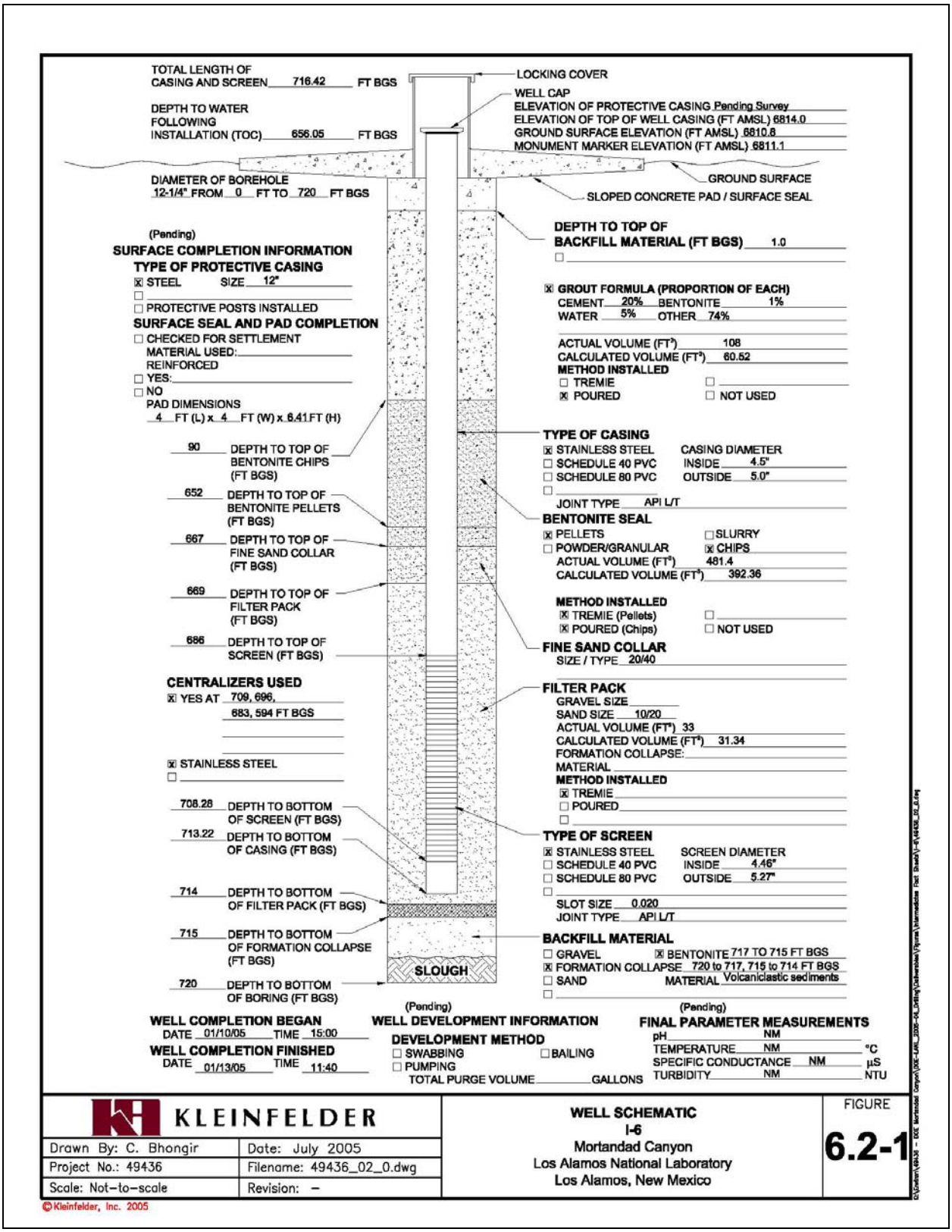

Figure 6.2-1. Well Schematic for I-6

7.0 WELL DEVELOPMENT, AQUIFER TESTING, AND PUMP INSTALLATION

7.1 Well Development

Development of I-6 began by bailing and swabbing the screened interval to enhance filter-pack settling and to remove drilling fluids and sediment that were introduced into the well during drilling and installation. Bailing was conducted with a 3.5-gal capacity, 3-in.-OD by 10-ft-long stainless-steel bailer. Swabbing was conducted by repeatedly drawing a swab across the screened interval. Approximately 92 gal. of water were removed during swabbing and bailing; 3,612 gal. were removed during well development and aquifer testing. Table 7.1-1 summarizes the volume of water removed during development to date and the total organic carbon concentration. Water quality parameters from additional development will be included in the final report.

Table 7.1-1
Water Removed and Water Quality Parameters
During Well Development

Method	Water Removed (gallons)	pH	Temp-erature (°C)	Specific Conductance (µS/cm)	Turbidity (NTU)	Total Organic Carbon (ppm)
Bailing/Swabbing	92	NM	NM	NM	NM	381
Pumping and Aquifer Testing	3,612	NM	NM	NM	NM	NM

µS/cm - microSiemens per centimeter
NM - not measured
NTU - nephelometric turbidity unit
ppm - parts per million

7.2 Aquifer Testing

Aquifer testing consisted of two trial tests per day on February 24 and February 25 and a constant-rate pumping and recovery test conducted from February 26 to 28. The complete aquifer testing report can be found in Appendix C. A 7.5-horsepower, 4-in.-diameter Grundfos submersible pump was used for aquifer testing. Additional well development occurred as the well was pumped during the aquifer testing. Multiple tests were conducted due to a malfunction in the check valves on the drop pipe drill string on February 24. It was necessary to remove the pumping string, replace the check valves, reinstall the pump, and restart the testing process.

The 24-hour constant-rate pumping test began at 8:30 A.M. on February 26. The well was pumped at 1.94 gallons per minute for 1,620 minutes. Recovery measurements were recorded for 1,266 minutes.

The following information summarizes the results of the pumping and recovery tests on I-6:

- Four short-duration trial tests and one 24-hour constant-rate pumping test were conducted.
- The lack of clear response of formation pressure (apparent hydrograph) to changes in barometric pressure implied a barometric efficiency of nearly 100%, consistent with what has been observed in most of the wells on the plateau.
- Casing storage effects were eliminated from the drawdown data sets. However, it appeared that a slow drainage event must have occurred during pumping because the water level rebound following pump shutoff was a result of storage effects. The effect was slight in the short tests, but significant in the 24-hour test.
- The transmissivity values calculated for the 8-ft-thick interflow zone were consistent, falling within a narrow range and averaging 64 gallons per day (gpd)/ft. The resulting average hydraulic conductivity was 8.0 gpd/ft^2, or 1.1 ft per day.
- Lower-bound transmissivity values obtained from specific capacity data and slug test responses averaged 57 gpd/ft, consistent with the transmissivity values obtained by conventional analysis.
- The data showed the effects of delayed yield associated with unconfined conditions.
- Water levels consistently failed to recover to the starting static water level after each pumping event, indicating a lateral limit to the perched zone or permeability reduction away from the well (or both). The latter scenario is likely, based on the low-transmissivity sediments in I-5 perched zone.
- The 24-hour pumping test showed unusual drainage-related responses that were probably related to saturated zone heterogeneities. It was possible that the drainage and refilling of discrete fractures or pockets of sediment caused the observed drawdown and recovery anomalies.

7.3 Dedicated Sampling System Installation

A dedicated sampling device is scheduled for installation in August 2005. The pump intake will be placed in the screened interval, with final design approval from DOE and LANL staff.

8.0 WELLHEAD COMPLETION, SURVEY, AND SITE RESTORATION ACTIVITIES

8.1 Wellhead Completion

A reinforced (2,500 psi) concrete pad, 4-ft wide by 4-ft long by 6.5-in. thick, was installed around the well casing to provide long-term structural integrity for the well. A brass survey cap was embedded in the northwest corner of the pad. A 10-in. diameter steel casing with locking lid protects the well riser. The pad was designed to be slightly elevated, with base course gravel graded up to the top of the pad.

8.2 Geodetic Survey

The abandoned corehole, ground surface, well casing, and brass cap of the I-6 borehole were surveyed by ASTS, Inc., in May 2005. The survey data are presented in Table 8.2-1.

Table 8.2-1
Geodetic Data

Description	Northing	Easting	Elevation*
Abandoned corehole	1768423.27	1635335.75	6810.5
Ground surface	1768429.56	1635345.2	6810.8
Brass cap in I-6 pad	1768428.06	1635345.65	6811.1
Top of stainless-steel casing	1768426.02	1635347.01	6814.0

*Measured in ft above mean sea level relative to the National Geodetic Vertical Datum of 1929

8.3 Site Restoration Activities

Fluids and cuttings produced during drilling and well development were sampled in accordance with the "Final Drilling Plan for Intermediate Wells" (Kleinfelder, 2004). Analytical results were received on March 4, 2005, and were submitted to DOE and LANL for review. A letter authorizing the discharge of cuttings and drilling and development water was received from the New Mexico Environment Department (NMED) on March 10, 2005.

Upon approval from NMED, investigation-derived water was spread over the site. The cuttings pit liner was removed, and containment area backfilled and leveled. The site has been reseeded.

9.0 DEVIATIONS FROM THE WORKPLAN

In general, drilling, sampling, and well construction at I-6 was performed as specified in the "Final Drilling Plan for Intermediate Wells, Mortandad Canyon" (Kleinfelder, 2004). However, the total depth of the borehole was 720 ft bgs rather than 760 ft bgs as noted in the work plan.

10.0 ACKNOWLEDGMENTS

EnviroWorks, Inc., provided site preparation services.

ASTS, Inc., conducted the final geodetic survey of finished well components.

Tetra Tech EM, Inc., provided support for site geology, sample collection, and aquifer testing.

WDC Exploration & Wells provided rotary drilling and well development services.

11.0 REFERENCES

Kleinfelder, 2004. "Final Drilling Plan for Intermediate Wells, Mortandad Canyon, Los Alamos National Laboratory," Los Alamos, New Mexico, Project No. 49436, October 2004.

Los Alamos National Laboratory, 2004. "Mortandad Canyon Groundwater Work Plan, Revision 1," Los Alamos National Laboratory Report LA-UR-0165, Los Alamos, New Mexico, January 2004.

Los Alamos National Laboratory, 2001. "Environmental Restoration Project Standard Operating Procedure for Well Construction, Revision 3," ER-SOP-5.01, April 2001.

Appendix A

Borehole Video Log

Appendix B

Lithologic Log

Appendix B - Lithologic Descriptions of Drill Cuttings in Borehole I-6

Geologic Unit	Lithologic Description	Sample Interval (ft)	Elevation Range (ft above msl)
Qal, Alluvium	No recovery. Sample not available for examination. **Note: Descriptions presented in this lithologic log are primarily based on observations made during visual examination of drill core and cuttings. From 0-498.2 ft bgs, lithologic description was generatad from drill core. Drill cuttings, collected on 5 foot intervals, were used from 498.2 ft to 720 ft bgs. Stratigraphic contacts are based on available information from review of drill core and limited geophysical logs. Unrecovered and/or sampled core in sections of less than 5 ft are not noted unless relevant to lithologic description.**	0-4	6810.8-6806.8
	Unconsolidated sediments, silty to very fine sand, moderate yellowish brown (10YR 5/4). Well-sorted (60% silt, 40% very fine sand); trace coarse sand size pumice fragments (subrounded); sand composed of tuff fragments, intermediate composition volcanic clasts (often rounded) with felsic (quartz and sanidine unless otherwise noted) crystals, faceted and bipyramidal; dry.	4-13.5	6806.8-6797.3
	Unconsolidated sediments, silty sand, moderate yellowish brown (10YR 5/4). Moderately sorted (20% silt, 20% fine sand, 40% medium sand, 10% coarse sand, 10% very coarse sand); felsic crystal rich (bipyramidal and faceted crystals); coarse sand to very coarse sand, intermediate composition volcanic clasts and pumice; dry.	13.5-20.5	6797.3-6790.3
	Unconsolidated sediments, as above; moist, slight increase in pumice percentage.	20.5-21.3	6790.3-6789.5
	Unconsolidated sediments, sandy silt, moderate yellowish brown (10YR 5/4). Well sorted (40% sand, 60% silt); subrounded to round sand; felsic crystal rich - frequent bipyramidal quartz, faceted crystal fragments; subround fine to medium sized welded tuff; trace fine gravel size intermediate composition volcanic clasts; dry.	21.3-27.5	6789.5-6783.3
	Unconsolidated sediments, sandy silt, pale yellowish brown (10YR 6/2). Well-sorted (10% coarse sand, 30% fine sand, 60% silt); trace felsic crystals, fine to coarse sand size; lithics and trace welded tuff, coarse sand-sized; dry.	27.5-28	6783.3-6782.8
	Unconsolidated sediments, sandy silt, pale brown (5YR 5/2). Moderately sorted (30% sand, 70% silt); highly weathered tuff, coarse sand to fine gravel sized, subrounded; felsic crystals, coarse sand to very coarse sand-sized fragments, subrounded to rounded, trace faceted surfaces; trace rootlets at 31.2 ft bgs; dry.	28-32.6	6782.8-6778.2
	Unconsolidated sediments, silts to very fine sand, light brown (5YR 6/4). Moderately sorted (70% silt, 30% sand); trace coarse to very coarse sand sized subrounded welded tuff fragments; dry. Grades to silty sand at 34.5 ft bgs predominantly coarse-grained, subrounded felsic crystals; moist.	32.6-34.5	6778.2-6776.3
	Unconsolidated sediments, silty to very fine sand, light brown (5YR 6/4). Moderately sorted (20% silt, 78% fine sand, 2% coarse to very coarse sand); trace coarse to very coarse sand-size felsic crystals, rounded; trace coarse sand to fine gravel sized welded tuff; trace rootlets; moist.	34.5-37.5	6776.3-6773.3
	Unconsolidated sediments, sandy gravel, moderate brown (5Y 5/6). Poorly sorted (60% gravel, 10% coarse sand, 20% fine sand, 10% very fine sand); felsic crystal sand matrix, subrounded; subrounded gravels, up to 3cm; moist.	37.5-38.5	6773.3-6772.3
	Unconsolidated sediments, silty sand, light brown (5YR 5/6) to moderate brown (5YR 4/4). Moderately sorted, predominantly coarse to very coarse sand; predominately felsic crystals (frequent bipyramidal quartz) and lesser amounts of intermediate composition volcanic clasts; trace welded tuff fragments to 5 cm; damp.	38.5-41.2	6772.3-6769.6
	Unconsolidated sediments, gravelly silt, moderate brown (5YR 4/4); wet.	41.2-42.5	6769.6-6786.3
	Unconsolidated sediments, silty sand, grayish brown (5YR 3/2). Poorly sorted (65-75% fine to coarse grained sand, 25-35% silt); felsic crystal rich, subrounded; 0-5% gravels to 10 mm, subrounded to subangular.	42.5-45	6786.3-6765.8
	Unconsolidated sediments, as above, grading to moderate brown (5YR 4/4), predominantly medium to coarse grained sand, moderately sorted, 90% felsic crystals with trace pumice and dark volcanic composition clasts; wet.	45-46.2	6765.8-6764.6
	Unconsolidated sediments, as above, grading to fine to medium grained silty sand, poorly sorted (0-5% gravel, 75-85% sand, 15/25% silt); rare dacite lithics; wet.	46.2-50.5	6764.5-6760.3
	Colluvium (weathered tuff) with unconsolidated sediments, grayish brown (5YR 3/2), poorly welded/unconsolidated. Tuff weathered to poorly graded sand with silt, fine to medium grained; felsic crystal rich; wet (saturated).	50.5-51.9	6760.3-6758.9
	Colluvium, as above, grading to silty sand, fine to coarse grained, poorly sorted (5-10% gravel, 60-70% sand, 20-35% fines); welded fragments > 40 mm with devitrified pumice to 5 mm, large felsic crystals; wet.	51.9-55.7	6758.9-6755.1
	Unconsolidated sediments, silty sand, pale brown (5YR 5/2). Welll sorted (5-10% gravel, 60-70% sand, 25-35% fines); fine grained sand, felsic crystals and minor intermediate composition volcanic clasts; tuff fragments up to 60 mm, felsic crystal rich, subrounded; wet (saturated).	55.7-59.4	6755.1-6751.4
	Unconsolidated sediments, silty sand, moderate brown (5YR 3/4). Poorly sorted (20-30% gravel, 50-60% sand, 20-30% fines); sand fine to coarse grained; tuff fragments > 50 mm, slightly to moderately weathered along tuff surface, pinkish gray, felsic crystal rich, frequent devitrified grayish pumice; wet.	59.4-63.2	6751.4-6747.6

Preliminary Log Compiled from Field Sample Descriptions (Revision A)

Geologic Unit	Lithologic Description	Sample Interval (ft)	Elevation Range (ft above msl)
	Colluvium (tuff), pale red (5R 6/2). Ash matrix; 25-35% felsic crystals; 5-15% devitrified pumice, up to 25 mm, aspect ratio 4:1; lithic poor; tuff surfaces and pumice slightly oxidized.	63.2-64.8	6747.6-6746.0
	Unconsolidated sediments, silty sand, grayish brown (5YR 3/2). Moderately sorted (0-5% gravel, 70-80% sand, 20-30% fines); predominantly fine grained sand, felsic crystals frequently rounded, bipyramidal quartz frequent; gravels to 10 mm, dacitic-andecitic clasts, subrounded;	64.8-68	6746.0-6472.8
	Unconsolidated sediments, as above, grading to fine grained, well sorted silty sand with clay, 25-35% silt content.	68-69.6	6472.8-6741.2
	Unconsolidated sediments, clayey sand with gravel, moderate brown (5YR 4/4). Moderately sorted, (30% clay and silt, 60% fine to very coarse sand, 10-15% gravels); predominantly fine grained matrix, felsic crystal rich, low to medium plasticity; dark subrounded gravels to 30 mm; wet (saturated)	69.6-73.2	6741.2-6737.6
	Unconsolidated sediments, silty clayey sand, moderate brown (5YR 4/4). Possible slough from 73.2 to 73.6 ft bgs. Poorly sorted, (30-40% fines, 40-50% sand, 5-10% gravel); low plasticity matrix; sand composed of very fine to medium grain size felsic crystals, subangular to rounded, 20% pumice fragments and lithics; gravel clasts up to 1 cm, composed of pumice and intermediate composition volcanic clasts; wet.	73.2-73.6	6737.6-6737.2
	Unconsolidated sediments, well sorted sand. Felsic crystal rich zone composed of: 15% felsic crystals (broken and faceted) increasing to 50% at 73.9 ft bgs; 25% intermediate volcanic composition clasts decreasing across interval; 10-15% tuff fragments, brown devitrified pumice; possible organic material at 74.3 ft bgs.	73.6-74.3	6737.2-6736.5
	Unconsolidated sediments, clayey sandy silt, moderate brown (5YR 4/4). Poorly sorted; sand predominately very fine to fine, trace felsic crystals, occasional faceted surfaces.	74.3-74.8	6736.5-6736.0
	Unconsolidated sediments, poorly sorted sand with minor fines. Felsic crystal rich zone; fine to very coarse felsic crystals, bipyramidal quartz.	74.8-75.3	6736.0-6735.5
Qct, Cerro Toledo Interval	Volcaniclastic sediments, sandy silt, light brown (5YR 5/6), unconsolidated. Poorly sorted sand composed of: 3-5% white vitric pumice, moisture altered, 3-5 mm, subrounded, rare hornblende phenocryst; 1-2% felsic crystals, small, rounded; rare obsidian fragment. **Note: The base of the alluvium/colluvium and the contact with the underlying Cerro Toledo Interval is interpreted to be at 75.3 ft bgs.**	75.3-75.7	6735.5-6735.1
	Volcaniclastic sediments, silty sand, moderate brown (5YR 4/4), unconsolidated. Moderately sorted; sands composed of 60% pumice fragments, 20-30% lithic clasts, 20% felsic crystals.	75.7-76.5	6735.1-6734.3
	Volcaniclastic sediments, silty sand, moderate brown (5YR 4/4), unconsolidated. Moderately sorted; sands composed of 60% pumice fragments, 20-30% lithic clasts, 20% felsic crystals.	76.5-76.9	6734.3-6733.9
	Volcaniclastic sediments, pumiceous sand with silt, grayish orange (10YR 7/4) to dark yellowish orange (10YR 6/6), unconsolidated. Moderately sorted (1% gravel, 84% sand, 15% fines); trace intermediate composition volcanic gravel clasts up to 1.0 cm; sand composed of predominately pumice, with 10-15% felsic crystals and 20-25% intermediate composition volcanic clasts,	76.9-78.8	6733.9-6732.0
	Volcaniclastic sediments, as above, poorly sorted, pale brown (5YR 5/2) to very pale orange (10YR 8/2); pumice slightly altered from moisture, noteable decrease in moisture content.	78.8-80.7	6732.0-6730.1
	Volcaniclastic sediments, gravelly sand, light brown (5YR 6/4) to grayish orange (10YR 7/4), unconsolidated. Moderately sorted, 30% poorly sorted gravels, predominately intermediate composition volcanic clasts, up to 3 cm and small pumice fragments; 50% poorly sorted sand, equal amounts of felsic crystals, pumice and lithic fragments; moist.	80.7-83.2	6730.1-6727.6
	Volcaniclastic sediments, pumiceous sand with gravel, pale yellowish brown (10YR 6/2), unconsolidated. Poorly sorted composed of 30-40% fine to coarse grained felsic crystals, 30-40% pumice fragments, 5-10% fine to coarse lithic clasts; 10-15% gravel, up to 3 cm; damp	83.2-86	6727.6-6724.8
	No recovery and/or core sampled. No core available for examination.	86-105	6724.8-6705.8
Qbo, Otowi Member of the Bandelier Tuff	Tuff, grayish orange (10YR 7/4), poorly welded. Ash matrix; 10-15% felsic crystals; 10-15% vitric pumice, up to 4 cm, felsic phenocrysts; 5-10% lithics, up to 10 mm, subrounded. **Note: The base of the Cerro Toledo Interval (Qct) and the contact with the underlying Otowi Member of the Bandelier Tuff (Qbo) is interpreted to be at 105 ft bgs.**	105-108	6795.8-6702.8
	Tuff, moderate reddish orange (10R 5/4), poorly welded. Ash matrix; 5-15% felsic crystals, fine to coarse grained; 10-15% pumice, up to 5 mm, white (N9), slightly weathered; 0-5% lithics, medium to coarse grained, subrounded.	108-113	6702.8-6697.8

Preliminary Log Compiled from Field Sample Descriptions (Revision A)

Geologic Unit	Lithologic Description	Sample Interval (ft)	Elevation Range (ft above msl)
	Tuff, moderate reddish orange (10R 5/4), poorly welded. Ash matrix; 10-15% felsic crystals decreasing percentage with depth, fine to medium grained; 0-5% pumice, up to 5 mm, vitric, white (N9), moderate weathering, 1:1 aspect ratio; 0-5% lithics, up to 40 mm, subangular to	113-118	6697.8-6692.8
	Tuff, moderate orange pink (10R 7/4) to moderate reddish orange (10R 6/6), poorly sorted. Ash matrix; 15-20% felsic crystals, medium to very coarse; 10-15% pumice, up to 25 mm, vitric, 2:1 to 1:1 aspect ratio, trace oxidation; 10-15% lithics, up to 20 mm, subrounded.	118-123	6692.8-6687.8
	Tuff, moderate orange pink (10R 7/4) to moderate reddish orange (10R 6/6), poorly welded. Ash matrix; 10-15% felsic crystals, fine to coarse grained; 5-10% pumice, up to 10 mm, 1:1 aspect ratio, vitric, felsic phenocrysts; 10-15% lithics, medium to coarse grained, subrounded.	123-128	6687.8-6682.8
	Tuff, moderate orange pink (10R 7/4) to moderate reddish orange (10R 6/6), poorly welded. Ash matrix; 20-25% felsic crystals, fine to coarse grained; 10-15% pumice, moderate reddish orange (10R 6/6), up to 2 cm, vitric, felsic phenocrysts; 10-15% lithics (dacite included) up to 1.5 cm, subrounded.	128-133	6682.8-6677.8
	Tuff, moderate orange pink (10R 7/4) to moderate reddish orange (10R 6/6), poorly welded. Ash matrix; 15-20% felsic crystals; 10-15% pumice, up to 20 mm, vitric, felsic phenocrysts; 15-20% lithics, subrounded.	133-136	6677.8-6674.8
	Tuff, moderate orange pink (10R 7/4) to light brown (5YR 5/6), poorly welded. Ash matrix; 20-25% felsic crystals; 10-15% vitric pumice, 1:1 aspect ratiio few 2:1, slight weathering along pumice surface; 15-20% lithics, up to 15 mm (including dacite), subrounded.	136-137.7	6674.8-6673.1
	Tuff, pale yellow orange (10YR 8/2), poorly welded. Ash matrix; 30-35% felsic crystals; pumice with felsic phenocrysts, rare mafic phenocrysts; 10-15% intermediate compostion volcanic lithics.	137.7-143	6673.1-6667.8
	Tuff, very pale orange (10YR 8/2) to grayish orange (10YR 7/4), poorly welded. Ash matrix; 15-20% felsic crystals; 15-20% lithics, up to 3 cm, subangular; 5-10% vitric pumice, up to 1 cm, occasional pumice up to 4 cm, 1:1 to 2:1 aspect ratio; moist.	143-153	6667.8-6657.8
	Tuff, very pale orange (10YR 8/2), poorly welded. Ash matrix; 20-30% fine to coarse felsic crystals; 5-15% dark yellow orange pumice, up to 3 cm, vitric with altered surfaces; 5- 10% dark lithics, up to 2 cm, at 156.1 ft bgs dacite lithic to greater than 50 mm, subangular.	153-163	6657.8-6647.8
	Tuff, very pale orange (10YR 8/2) to grayish orange (10YR 7/4), poorly welded. Ash matrix; 20-30% felsic crystals; 20-30% vitric pumice, up to 3 cm, trace weathered and altered; 5-15% lithics, up to 1 cm	163-180.7	6647.8-6630.1
	Tuff, pale yellowish brown (10YR 6/2). poorly welded. Ash matrix; 5-15% felsic crystals; 0-15% pumice, up to 5 cm, vitric, silghtly weathered, felsic phenocrysts; 0-5% lithic up to 1 cm, subrounded	180.7-203	6630.1-6607.8
	Tuff, pale yellowish brown (10YR 6/2), poorly welded. Ash matrix; 5-10% felsic crystals, very fine to medium grained; 0-5% pumice, vitric, up to 2 cm, aspect ratio 1:1; 0-5% lithics, up to 3 cm, subrounded	203-208	6607.8-6602.8
	Tuff, pale yellowish brown (10YR 6/2), poorly welded. Ash matrix; 5-15% felsic crystals, predominantly quartz, very fine to medium grained; 0-5% pumice, vitric, up to 3 cm, felsic phenocrysts; 5-10% lithics, up to 4 cm, subangular to subrounded; possible altered mica flecks,	208-213	6602.8-6597.8
	Tuff, pale yellowish brown (10YR 6/2), poorly welded. Ash matrix; 5-10% felsic crystals; 0-5% pumice, up to 1 cm, aspect ratio 1:1, vitric, felsic phenocrysts; 5-10% lithics, up to 2 cm, subangular to subrounded, pumice pale yellowish orange (10YR 8/6) to dark yellowish orange	213-223	6597.8-6587.8
	Tuff, pale yellowish brown (10YR 6/2), poorly welded. Ash matrix; 5-10% felsic crystals; 0-5% pumice, dark yellowish orange (10YR 6/6), up to 2 cm, aspect ratio 1:1 to 2:1, vitric, felsic phenocrysts; 0-5% lithics, subrounded.	223-228	6587.8-6582.8
	Tuff, pale yellow brown (10YR 6/2), poorly welded. Ash matrix; 10-15% felsic crystals; 5-10% vitric pumice, up to 2 cm, dark yellowish orange (10YR 6/6), aspect ratio 1:1 to 2:1, felsic phenocrysts, alteration and weathering along pumice surfaces; 0-5% lithics, up to 5 cm intermediate composition volcanic clasts, subrounded to subangular; high angle fractures at 230.5 ft and 233 ft bgs, clay coated surfaces.	228-243	6582.8-6567.8
	Tuff, pale yellowish brown (10YR 6/2), poorly welded. Ash matrix; 15-25% felsic crystals; 10-15% vitric pumice, up to 2 cm, apsect ratio of 2:1 to 1:1, dark yellowish orange, felsic phenocrysts, altered pumice surfaces; 5-10% lithics, up to 1 cm, subrounded.	243-260	6567.8-6550.0
	Tuff, pale yellowish brown (10YR 6/2) to moderate yellowish brown (10YR 5/4), poorly welded. Ash matrix; 10-20% felsic crystals; 10-20% vitric pumice, up to 2 cm, occasional up to 6 cm, dark yellowish orange to moderate orange, felsic phenocrysts, absence of weathering on pumice surfaces, aspect ratios predominantly 2:1; 5-15% lithics, up to 0.5 cm, subrounded to subangular.	260-280	6550.8-6530.8
	Tuff, very pale orange (10YR 8/2) to pale yellowish brown (10YR 6/2), poorly welded. Ash matrix; 0-10% felsic crystals; 0-5% pumice, up to 2.5 cm, vitric, minor oxidation and alteration of the pumice fibers, larger pumice have felsic phenocrysts; 0-5% lithics, subrounded; 0-2% mafics fragments.	280-293	6530.8-6517.8
	Tuff, very pale orange (10YR 8/2) to pale yellowish brown (10YR 6/2), poorly welded. Ash matrix; 0-10% felsic crystals; 0-5% pumice, vitric, trace alteration, up to 2.0 cm, aspect ratio 1:1, felsic phenocrysts; 0-5% lithics, up to 1.5 cm, subangular to subrounded.	293-312	6517.8-6498.8
	Tuff, pale yellowish brown (10 YR 6/2), poorly welded. Ash matrix; 3% pumice, white (N9), 2 mm to 1 cm, vitric, fibrous, felsic phenocrysts, rare mafic phenocrysts and surficial Mn/Fe oxide specks; 3% lithics, up to 1cm, subrounded to rounded; 7% felsic crystals; moist.	312-326	6498.8-6484.8
	Tuff, as above, decrease in average pumice size (1-5 mm); decrease in felsic crystals to 5%; dry.	326-327.1	6484.8-6483.7
	Tuff, pale yellowish brown (10YR 6/2), poorly welded. Ash matrix; 3% pumice, white (N9) to yellowish brown, 2 mm to 1.5 cm, vitric, subhedral felsic phenocrysts; 3-7% felsic crystals (in matrix) are medium to coarse sized, subhedral; 3% lithics, subrounded to rounded, coarse sand to granule to rarely gravel-sized; intermediate composition volcanic lithics; moist.	327.1-341	6483.7-6469.8
	Tuff, pale yellowish brown (10YR 6/2), poorly welded. Ash matrix; 2-5% pumice, white (N9), 1 mm to 2 cm, vitric, subhedral felsic phenocrysts, surficial Mn/Fe specks; 3-7% felsic crystals (in matrix), subhedral; 2-5% lithics, subrounded to rounded, coarse sand to granule to rarely gravel-sized, intermediate composition volcanics; moist.	341-361.9	6469.8-6448.9
	Tuff, pale yellowish brown (10YR 6/2), poorly welded. Ash matrix; 2-5% pumice, white (N9), 1 mm to 2 cm, vitric, fibrous, subhedral mafic felsic phenocrysts, trace Mn/Fe oxide staining; 3-7% felsic crystals, coarse sand sized, subhedral; 2-5% lithics, subrounded to rounded, coarse sand to granule to rarely gravel-sized; moist.	361.9-402	6448.9-6408.8
	Tuff, pale yellowish brown (10YR 6/2), poorly welded. Ash matrix; 2-5% pumice, white (N9), 1 mm to 2 cm, vitric, rare mafic and felsic phenocrysts, occasional surficial Mn/Fe specks; 3-7% felsic crystals are coarse sand sized, subhedral; 2-5% lithics, subrounded to rounded, coarse sand to granule to rarely gravel-sized; moist.	402-423	6408.8-6387.8
	Tuff, pale yellowish brown (10YR 6/2), poorly welded. Ash matrix; 2-5% pumice, white (N9), 1 mm to 2 cm, vitric, fibrous, coarse sand sized subhedral felsic phenocrysts; 3-7% felsic crystals, coarse sand sized, subhedral; 2-5% lithics, subrounded to rounded, coarse sand to granule to rarely gravel-sized; moist, minor alteration due to moisture.	423-433	6387.8-6377.8
	Tuff, as above, marked increase in pumice to 60%.	433-434.4	6377.8-6376.4
Qbog, Guaje Pumice Bed of the Otowi Member of the Bandelier Tuff	Pumice Bed, very light gray (N8), poorly welded. 60-80% pumice, white (N9), 2 mm to 2.5 cm, vitric, coarse subhedral felsic phenocrysts, very rare subhedral mafic phenocrysts(<1mm); 10-20% felsic crystals; 2-5% lithics, coarse sand to rarely granule or gravel-sized, subrounded to rounded; moist. **Note: The base of the Otowi Member of the Bandelier Tuff (Qbo) and the contact with the underlying Guaje Pumice Bed (Qbog) is interpreted to be at 434.3 ft bgs.**	434.4-447	6376.4-6363.8
	Pumice Bed, as above, pumice increase up to 95%, average size increase with depth.	447-450.5	6363.8-6360.3

Preliminary Log Compiled from Field Sample Descriptions (Revision A)

Geologic Unit	Lithologic Description	Sample Interval (ft)	Elevation Range (ft above msl)
Tpf, Puye Formation (fanglomerate)	Volcaniclastic sediments, clayey silt with sand, moderate yellowish brown (10YR 5/4), moderately consolidated. Very well sorted (0% gravel, 1% sand, 99% fines); very thin (0.5 cm) layer of clay altered ash at top of formation, moist. **Note: The base of the Guaje Pumice Bed (Qbog) and the contact with the underlying Puye Formation (Tpf) is interpreted to be at 450.5 ft bgs.**	450.5-453	6360.3-6357.8
	Volcaniclastic sediments, as above, decrease in clay and silt percentage (50-70%), increase in fine sand (30-50%) and appearance of rare coarse sand gravel (0-2%), intermediate composition volcanic clasts and pumice (0-1%) with depth.	453-463	6357.8-6347.8
	Volcaniclastic sediments, sandy silty gravel, moderate yellowish brown (10YR 5/4), unconsolidated. Poorly sorted (50-70% gravel, 25-45% sand, 5% fines); felsic crystal rich; intermediate composition volcanic clasts, very coarse gravel up to 4 cm; rare pumice;	463-468.8	6347.8-6342.0
	As above; with large dacite clast, dark gray, approximately 10 mm, frequent feldspar phenocrysts.	468.8-469.9	6342.0-6340.9
	No recovery and/or core sampled. No core available for examination.	469.9-493	6340.9-6317.8
Tb, Cerros del Rio Basalt	Basalt, medium light gray (N6), highly vesicular. Aphanitic groundmass, 2% olivine phenocrysts; moist in sample tube. At 496 ft bgs, large, single white crystal growth; at 497.5 ft bgs, near-horizontal fracture with clay-lined aperature. **Note: The base of the Puye Formation (Tpf) and the contact with the underlying Cerros del Rio Basalt (Tb) is interpreted to be at 493 ft bgs.**	493-498.2	6317.8-6312.6
	Basalt; medium light gray (N5), intermixing of cuttings with overlying formation. WR (whole rock, unsieved): basalt chips coated with very pale orange (10YR, 8/2) fines. 10+F (i.e. plus No. 10 sieve-size fraction): 50% basalt, vesicular, frequently oxidized/altered pit linings, up to 1.5 cm, subangular to subrounded; 50% intermediate composition volcanic clasts, hornblende dacite frequent, up to 1.5 cm, subangular to subrounded. 35+F(i.e. plus No. 35 sieve-size fraction): very poor returns. **Note: from 495 ft bgs to 720 ft bgs, lithologic description generated from drill cuttings.**	498.2-500	6312.6-6310.8
	Basalt, medium gray (N5) to medium dark gray (N4), vesicular. WR: 90% fragments of basalt with minor siltstone and fines. 10+F: 95% basalt chips, vesicular, medium gray, 1-2% olivine phenocyst, minor clay lining of pits, slightly granular texture; 1-2% siltstone fragments; 1-2% white, vitric pumices; 1-2% lithics, up to 2 cm, angular to subrounded. 35+F: finer fraction as described for 10+F, plus 5-10% felsic crystals, occasional faceted surface.	500-510	6310.8-6300.8
	Basalt; brownish gray (5YR 4/1) to grayish red (10R 4/2), massive to vesicular. 10+F: basalt chips, grayish red to brownish gray, alteration of vesicules decreasing across interval, moderate reddish brown (10R 4/6) staining and vesicular basalt predominant from 515-520 ft bgs. 35+F: finer fraction as described for 10+F with 2-5% felsic crystals.	510-530	6300.8-6280.8
	Basalt; brownish gray (5YR 4/1), massive with minor vesicles; WR: basalt chips with trace fines coating. 10+F basalt chips, up to 1 cm, broken fragments, massive, trace vesicles, minor alteration, slightly granular texture, 1-2% olivine phenocrysts. 35+F finer fraction as described for 10+F, plus 2-5% felsic crystals.	530-550	6280.8-6260.8
	Basalt, as above, slight color change to medium light gray (N6).	550-560	6260.8-6250.8
	Basalt; medium dark gray (N4) to grayish black (N2), minor alteration to grayish olivine green (5GY 3/2), massive. 10+F: basalt, massive, minor alteration, fragments up to 2 cm, angular. 35+F: as for 10+F, finer fraction.	560-570	6250.8-6240.8
	Poor, intermixed returns.	570-575	6240.8-6235.8
	Basalt, medium gray (N5), massive. 10+F: basalt chips up to 1.5 cm, angular, 1-2% olivine (green to reddish brown) phenocrysts, microcrystalline (granular texture) to aphanitic; trace alteration; trace clay fragments beginning at 590 ft bgs. 35+F: finer fraction as described for 10+F, plus minor pumice and very fine felsic fragments.	575-600	6235.8-6210.8
	Basalt, medium gray (N5), massive. 10+F: basalt fragments up to 2 cm, angular, granular to aphanitic texture, 1-2% olivine (green to reddish brown) phenocrysts; trace (2-3%) sandstone/clay fragments, lamination present, minor alteration of fragments. 35+F: finer fraction	600-610	6210.8-6200.8
	Basalt with mixed returns, including pumice, felsic crystals; predominantly medium dark gray (N4), massive to vesicular basalt. 10+F: basalt, massive, slightly granular, gray fragments approximately 65% decreasing to 40% across interval, 1-2% olivine phenocrysts; vesicular, reddish brown fragments approximately 35% increasing to 50% across interval, frequently altered, clay lined pits; 0-5% pumice, white, vitric; 1-5% sandstone/clay fragments; trace lithics (subrounded). 35+F: 35-40% felsic crystals decreasing to trace at 620 ft bgs, fine grain-size; finer fraction as described for 10+F.	610-625	6200.8-6185.8
	Basalt; grayish black (N2) to very dusky red (10R 2/2), massive and vesicular. 10+F: basalt, massive and vesicular fragments, 1-2% olivine phenocrysts, trace clay fragments. 35+F: finer fraction as described for 10+F.	625-630	6185.8-6180.8
	Poor returns - similar returns to 610-625 feet interval.	630-635	6180.8-6175.8
	Basalt, brownish gray (5YR 4/1), massive. 10+F: basalt, massive, slightly vesicular, 1-2% dark reddish brown olivine phenocrysts, slightly granular texture. 35+F: finer fraction as described for 10+F; plus 2-5% felsic, occasional faceted surface; trace clay fragments/pumice.	635-650	6175.8-6160.8
	Basalt with minor returns of felsic crystals, silt/clay and pumice fragments; basalt, dark gray (N3), massive, minor vesicles. 10+F: 98% basalt fragments, massive with minor vesicles, 1-2% dark reddish brown to green olivine phenocrysts, occasional clay infill of pits and lining of surfaces; 2% clay fragments and vitric pumices; up to 1 cm, angular. 35+F: 10-25% felsic crystals, occasional faceted surfaces; 75% basalt as described for 10+F.	650-665	6160.8-6145.8
	Basalt with minor returns of felsic crystals, silt/clay and pumice fragments; basalt, black (N1) to dark gray (N3); massive to weakly vesicular; fresh, clean appearance. 10+F: basalt, massive to weakly vesicular, minor clay lining on fragments, dark gray to black, very fine grained groundmass, 2-3% phenocrysts, including olivine, dark gray to dark reddish brown; 5-10% clay fragments. 35+F: finer fraction as described for 10+F with minor free felsic crystals.	665-680	6145.8-6130.8
	Basalt with minor fines, medium dark gray (N3). WR: massive basalt with trace yellowish gray fines. 10+F: basalt fragments, up to 2 cm, massive with 0-2% altered vesicles, aphanitic, 1-2% phenocrysts, olivine noted; 2-5% clay fragments; trace free felsic crystals. 35+F: finer fractions as described for 10+F, 60-70% basalt, 15-20% clay fragments, 10-15% free felsic crystals, occasional faceted surface.	680-695	6130.8-6115.8
	Basalt with minor fines, medium dark gray (N3). WR: massive basalt with trace yellowish gray (5Y 8/1) fines. 10+F: basalt fragments, up to 2 cm, massive, aphanitic, 1% olivine phenocrysts; 2-5% clay fragments; free felsic crystal fragments at 695-700 ft bgs. 35+F: variable percentages of free felsic crystals (occasional faceted surface), basalt chips, and clay fragments.	695-710	6115.8-6100.8
	Basalt, medium dark gray (N3). WR: massive and vesicular fragments with rare fines. 10+F: 98% basalt, massive fragments up to 1.5 cm, microcrystalline to aphanitic, 1-2% olivine phenocrysts; 2% vesicular basalt, aphanitic, clay lining; trace lithic clast - likely displaced. 35+F: 65-80% basalt chips; 10-15% clay fragments; 30-35% felsic crystals, occasional faceted surface.	710-720	6100.8-6090.8
	TOTAL BOREHOLE DEPTH (TD) IS AT 720 FT BGS.		

NOTES:

Descriptions presented in this lithologic log are primarily based on observations made during visual examination of drill core and cuttings. From 0- 498.2 ft bgs, lithologic description was generated from drill core. Drill cuttings, collected on 5 foot intervals, were used from 498.2 ft to 720 ft bgs. Unrecovered and/or sampled core in sections of less than 5 ft are not noted unless relevant to lithologic description.

Stratigraphic contacts are based on available information from review of drill core and limited geophysical logs. There is general agreement between this borehole log and the geophysics report.

Descriptions of drill chips and drill core from sedimentary units such as the Quaternary Alluvium, Cerro Toledo Interval and the Puye Formation utilized principles outlined in *Petrology of Sedimentary Rocks* by Robert L. Folk. Color Descriptions were determined using The Geological Society of America, Rock-Color Chart.

Geologic Unit	Lithologic Description	Sample Interval (ft)	Elevation Range (ft above msl)

Cuttings were collected at nominal 5 or 10 ft intervals and divided into three sample splits: (1) unsieved, or whole rock (WR), sample; (2) 10+F sieved fraction (No. 10 sieve equivalent to 2.0 mm); and (3) 35+F sieved fraction (No. 35 sieve equivalent to 0.5 mm). When cuttings were overall finer grained, then cuttings were divided into a 35+F sieved fraction and a 60+F sieved fraction.

Fractures were visually inspected for an approximate orientation. The angle of the fracture surface is approximated from vertical.

The term "percent" (%), as used in the above descriptions, refers to the visual estimate of the relative abundance by volume for a given sample component.

REFERENCES:

Folk, Robert L., 1980, *Petrology of Sedimentary Rocks* , Hemphill Publishing Company.
The Geological Society of America, 1991, Rock-Color Chart.

Appendix C

Aquifer Testing Report

I-6 PUMPING TEST ANALYSIS

Introduction

This section describes the analysis of constant-rate pumping tests conducted in February 2005 on intermediate well I-6, located in Mortandad Canyon, not far from R-15 and I-5. The primary objective of the analysis was to determine the hydraulic properties of the saturated sediments screened in I-6. Consistent with the protocol used in most of the R-well pumping tests, the I-6 testing incorporated an inflatable packer above the pump to minimize barometric effects and eliminate the effects of casing storage on the measured data. Packer implementation was partially successful in minimizing storage effects.

I-6 is completed with a single screen, 22 feet long, in a perched zone within the Cerros del Rio basalt a few hundred feet above the regional aquifer, between the depths of 686 and 708 feet. The perched water level lies 24 feet above the top of the well screen, at approximately 662 feet below land surface.

The saturated zone consists of alternate layers of basalt and porous interflow breccias. According to geophysical logs, there are massive, presumably tight, basalt flows from 686 to 692 feet (top 6 feet of well screen) and 700 to 715 feet (overlapping the bottom 8 feet of well screen). The deeper basalt flow may form the perching unit at this location. The screened aquifer was considered to be the 8-foot-thick interflow zone from 692 to 700 feet between the massive basalt flows. It was expected that there were additional permeable interflow zones above the screened interval as well, but the degree of their hydraulic connection to the pumped zone was uncertain, because of the intervening basalt flow.

Testing consisted of two trial tests on February 24, two more trials on February 25 and a constant-rate pumping and recovery test conducted from February 26 to 28. The reason for the multiple trial tests was that the check valves in the drop pipe string failed following the February 24 testing. Therefore, it was necessary to remove the pumping string, replace the check valves, reinstall the pump and restart the testing process.

The first trial tests were conducted after the pump was installed on February 24. In trial 1, the well was pumped at 1.83 gpm for 69 minutes from 3:14 pm to 4:23 pm, followed by 120 minutes of recovery until 6:23 pm. In trial 2, the well was pumped at multiple flow rates, averaging 1.7 gpm, for 117 minutes from 6:23 pm to 8:20 pm, followed by 908 minutes of recovery until packer deflation at 11:28 am on February 25.

Following confirmation that the check valves had failed, the pump was removed and reinstalled, and two additional trial tests were performed. In trial 3, the well was pumped at 1.8 gpm for 20 minutes from 3:41 pm to 4:01 pm, followed by 70 minutes of recovery until 5:11 pm. In trial 4, the well was pumped at 1.84 gpm for 71 minutes from 5:11 pm to 6:22 pm, followed by 848 minutes of recovery until initiation of the constant-rate test at 8:30 am on February 26.

The 24-hour constant-rate pumping test was begun at 8:30 am on February 26. The well was pumped at 1.94 gpm for 1620 minutes until 11:30 am on February 27. Following pump shutoff, water level recovery data were recorded for 1266 minutes until 8:36 am on February 28. The

extended recovery data that followed the constant-rate test and each day of trial testing also served as background data.

Background Data

The background water level data collected in conjunction with running the pumping tests allow the analyst to see what water level fluctuations occur naturally in the saturated zone and help distinguish between water level changes caused by conducting the pumping test and changes associated with other causes.

Background water level fluctuations have several causes, among them barometric pressure changes, operation of other wells, earth tides and long-term trends related to weather patterns. The background data hydrographs from the I-6 tests were compared to barometric pressure data from the area to determine if a correlation existed.

Previous pumping tests have demonstrated a barometric efficiency for most wells of between 90 and 100 percent. Barometric efficiency is defined as the ratio of water level change divided by barometric pressure change, expressed as a percentage. In the initial pumping tests conducted as part of this project, down hole pressure was monitored using a *vented* transducer. This equipment measures the *difference* between the total pressure applied to the transducer and the barometric pressure, this difference being the true height of water above the transducer.

Subsequent pumping tests, including I-6, have utilized a *non-vented* transducer. This device simply records the total pressure on the transducer, that is, the sum of the water height plus the barometric pressure. This results in an attenuated "apparent" hydrograph, rather than a true hydrograph, in a barometrically efficient well. Take as an example a 90 percent barometrically efficient well. When monitored using a vented transducer, an *increase* in barometric pressure of 1 unit causes a *decrease* in recorded down-hole pressure of 0.9 units, because the water level is forced downward 0.9 units by the barometric pressure change. However, using a non-vented transducer, the total measured pressure *increases* by 0.1 units (the combination of the barometric pressure increase and the water level decrease). Thus, the resulting apparent hydrograph changes by a factor of 100 minus the barometric efficiency, and in the same direction as the barometric pressure change, rather than in the opposite direction.

Barometric pressure data were obtained from the Los Alamos National Laboratory TA-54 tower site from RRES-Meteorology and Air Quality. The TA-54 measurement location is at an elevation of 6548 feet above mean sea level (amsl), whereas the wellhead elevation was approximately 6850 feet amsl. Furthermore, the static water level in I-6 was about 662 feet below land surface, making the water table elevation approximately 6188 feet amsl. Therefore, the measured barometric pressure data from TA-54 had to be adjusted to reflect the pressure at the elevation of the water table within I-6.

The following formula was used to adjust the measured barometric pressure data:

$$P_{WT} = P_{TA54} \exp\left[-\frac{g}{3.281R}\left(\frac{E_{I6} - E_{TA54}}{T_{TA54}} + \frac{E_{WT} - E_{I6}}{T_{WELL}} \right) \right],$$

where

P_{WT} = barometric pressure at the water table inside I-6
P_{TA54} = barometric pressure measured at TA-54
g = acceleration of gravity, in m/sec^2 (9.80665 m/sec^2)
R = gas constant, in J/Kg/degree Kelvin (287.04 J/Kg/degree Kelvin)
E_{I6} = land surface elevation at I-6, in feet (approximately 6850 feet)
E_{TA54} = elevation of barometric pressure measuring point at TA-54, in feet (6548 feet)
E_{WT} = elevation of the water level in I-6, in feet (6188 feet)
T_{TA54} = air temperature near TA-54, in degrees Kelvin (assigned a value of 33.4 degrees Fahrenheit, or 273.9 degrees Kelvin)
T_{WELL} = air temperature inside I-6, in degrees Kelvin (assigned a value of 56.7 degrees Fahrenheit, or 286.9 degrees Kelvin)

This formula is an adaptation of an equation provided by RRES-Meteorology and Air Quality. It can be derived from the ideal gas law and standard physics principles. An inherent assumption in the derivation of the equation is that the air temperature between TA-54 and the well is temporally and spatially constant, and that the temperature of the air column in the well is similarly constant.

The corrected barometric pressure data reflecting pressure conditions at the water table were compared to the water level hydrograph to discern the correlation between the two.

Early Data Response

In many low-yield pumping tests, such as those conducted in the monitoring wells on the plateau, casing storage effects dominate the early-time data, hindering the data analysis. The duration of casing storage effects can be estimated using the following equation (Schafer, 1978).

$$t_c = \frac{0.6\left(D^2 - d^2\right)}{\frac{Q}{s}},$$

where

t_c = duration of casing storage effect, in minutes
D = inside diameter of well casing, in inches
d = outside diameter of column pipe, in inches
Q = discharge rate, in gpm
s = drawdown observed in pumped well at time t_c, in feet

In some instances, it is possible to eliminate casing storage effects by setting an inflatable packer above the tested screen interval prior to conducting the test. Therefore, this option has been implemented for the R-well testing program, including the I-6 pumping test.

Time-Drawdown Methods

Time-drawdown data can be analyzed using a variety of methods. Among them is the Theis method. The Theis equation describes drawdown around a well as follows:

$$s = \frac{114.6Q}{T} W(u),$$

where

$$W(u) = \int_u^\infty \frac{e^{-x}}{x} dx$$

and

$$u = \frac{1.87 r^2 S}{Tt}$$

and where

s = drawdown, in feet
Q = discharge rate, in gpm
T = transmissivity, in gpd/ft
S = storage coefficient (dimensionless)
t = pumping time, in days
r = distance from center of pumpage, in feet

To use the Theis method of analysis, the time-drawdown data are plotted on log-log graph paper. Then, Theis curve matching is performed using the Theis type curve – a plot of the Theis well function $W(u)$ versus $1/u$. Curve matching is accomplished by overlaying the type curve on the data plot and, while keeping the coordinate axes of the two plots parallel, shifting the data plot to align with the type curve, effecting a match position. An arbitrary point, referred to as the match point, is selected from the overlapping parts of the plots. Match point coordinates are recorded from the two graphs, yielding four values – $W(u)$, $1/u$, s and t. Using these match point values, transmissivity and storage coefficient are computed as follows:

$$T = \frac{114.6Q}{s} W(u) \text{ and}$$

$$S = \frac{Tut}{2693 r^2},$$

where

T = transmissivity, in gpd/ft
S = storage coefficient
Q = discharge rate, in gpm

$W(u)$ = match point value
s = match point value, in feet
u = match point value
t = match point value, in minutes

An alternative solution method applicable to time-drawdown data is the Cooper-Jacob method (1946), a simplification of the Theis equation (1935) that is mathematically equivalent to the Theis equation for most pumped well data. The Cooper-Jacob equation describes drawdown around a pumping well as follows:

$$s = \frac{264Q}{T} \log \frac{0.3Tt}{r^2 S},$$

where

s = drawdown, in feet
Q = discharge rate, in gpm
T = transmissivity, in gpd/ft
t = pumping time, in days
r = distance from center of pumpage, in feet
S = storage coefficient (dimensionless)

The Cooper-Jacob equation is a simplified approximation of the Theis equation and is valid whenever the u value is less than about 0.05.

For small radius values (e.g., corresponding to borehole radii), u is less than 0.05 at very early pumping times and, therefore, is less than 0.05 for nearly all measured drawdown values. Thus, for pumped wells, the Cooper-Jacob equation usually can be considered a valid approximation of the Theis equation. (Note: an exception to this can occur when the transmissivity is exceedingly low. If the transmissivity is sufficiently small, some of the very early time measurements may not meet the u-value criterion, even in the pumped well.)

According to the Cooper-Jacob method, the time-drawdown data are plotted on a semilog graph, with time plotted on the logarithmic scale. Then a straight line of best fit is constructed through the data points and transmissivity is calculated using:

$$T = \frac{264Q}{\Delta s},$$

where

T = transmissivity, in gpd/ft
Q = discharge rate, in gpm
Δs = change in head over one log cycle of the graph, in feet

The Neuman (1974) method for a partially penetrating well in an unconfined aquifer also was applied to the drawdown data to account for partial penetration effects. This analysis was

performed to see if the results were consistent with other analyses. The Neuman equation expresses drawdown in a partially penetrating well in an unconfined aquifer as follows:

$$s = \frac{Q}{4\pi T}\int_0^\infty 4yJ_0\left(y\sqrt{\beta}\right)\left[u_0(y)+\sum_{n=1}^{\infty}u_n(y)\right]dy,$$

where

$$\beta = \frac{r^2K_z}{b^2K_r}$$

$$\sigma = \frac{S}{S_y}$$

$$u_0(y) = \frac{\left\{1-\exp\left[-t_s\beta\left(y^2-\gamma_0^2\right)\right]\right\}\left\{\sinh\left(\gamma_0 z_{2D}\right)-\sinh\left(\gamma_0 z_{1D}\right)\right\}}{\left\{y^2+(1+\sigma)\gamma_0^2-\left(y^2-\gamma_0^2\right)^2/\sigma\right\}\cosh\left(\gamma_0\right)}\cdot$$

$$\frac{\sinh\left[\gamma_0(1-d_D)\right]-\sinh\left[\gamma_0(1-l_D)\right]}{\left(z_{2D}-z_{1D}\right)\gamma_0\left(l_D-d_D\right)\sin\left(\gamma_0\right)}$$

$$u_n(y) = \frac{\left\{1-\exp\left[-t_s\beta\left(y^2+\gamma_n^2\right)\right]\right\}\left\{\sinh\left(\gamma_n z_{2D}\right)-\sinh\left(\gamma_n z_{1D}\right)\right\}}{\left\{y^2-(1+\sigma)\gamma_n^2-\left(y^2+\gamma_n^2\right)^2/\sigma\right\}\cosh\left(\gamma_n\right)}\cdot$$

$$\frac{\sinh\left[\gamma_n(1-d_D)\right]-\sinh\left[\gamma_n(1-l_D)\right]}{\left(z_{2D}-z_{1D}\right)\gamma_n\left(l_D-d_D\right)\sin\left(\gamma_n\right)}$$

The gamma terms are the roots of the following equations:

$$\sigma\gamma_0\sinh\left(\gamma_0\right)-\left(y^2-\gamma_0^2\right)\cosh\left(\gamma_0\right)=0,\gamma_0^2<y^2$$

and

$$\sigma\gamma_n\sin\left(\gamma_n\right)+\left(y^2-\gamma_n^2\right)\cos\left(\gamma_n\right)=0,(2n-1)/(\pi/2)<\gamma_n<n\pi,n>=1.$$

In these equations, the parameters are defined as follows:

b = aquifer thickness
d_D = vertical distance between top of pumping well screen and initial water table divided by the aquifer thickness
J_0 = Bessel function of first kind, zero order
K_r = horizontal hydraulic conductivity

K_z = vertical hydraulic conductivity
l_D = vertical distance between bottom of pumping well screen and initial water table divided by the aquifer thickness
r = radial distance
S = elastic storage coefficient
S_y = specific yield
t_s = dimensionless time with respect to specific storage, equal to Tt/Sr^2
t = recovery time
T = transmissivity
z_{1D} = vertical distance from bottom of aquifer to bottom of observation well screen divided by aquifer thickness
z_{2D} = vertical distance from bottom of aquifer to top of observation well screen divided by aquifer thickness

A potential advantage of the Neuman method is that it accounts for both partial penetration and vertical movement of the water table in an unconfined aquifer, as the sediments drain and re-saturate during pumping and recovery. A disadvantage of this method is that the complex equations are difficult to solve, are non-intuitive, and often lead to bizarre or impossible solutions of parameter combinations. As a consequence, it is particularly important to closely scrutinize output from the Neuman solution method.

Recovery Methods

Recovery data were analyzed by the Theis Recovery Method. This is a semi-log analysis method similar to the Cooper-Jacob procedure.

In this method, residual drawdown is plotted on a semi-log graph versus the ratio t/t', where t is the time since pumping began and t' is the time since pumping stopped. A straight line of best fit is constructed through the data points and T is calculated from the slope of the line as follows:

$$T = \frac{264Q}{\Delta s}.$$

The recovery data are particularly useful compared to time-drawdown data. Because the pump is not running, spurious data responses associated with dynamic discharge rate fluctuations are eliminated. The result is that the data set is generally "smoother" and easier to analyze.

Theis curve matching also was applied to the recovery data. This was done by plotting recovery time versus feet of recovery (difference between the maximum drawdown observed at the end of the pumping test and the residual drawdown) and performing curve matching analogous to the time-drawdown method. This method of analysis is valid for early recovery time.

Slug Test Methods

During the testing of I-6, water leaked out of the 1-inch drop pipe into the annulus between the drop pipe and the 4.5-inch ID well casing. It is likely that the leaks occurred through the coupling joints. However, in previous tests where this occurred, the drop pipe was found to have

a defective weld seam, allowing water to leak directly through the pipe itself, so this could have been the cause also. After test pumping, when the packer was deflated, the accumulated water above the packer was delivered to the well rapidly, similar to a slug test stress. Therefore, slug test methods were used to analyze this event in I-6.

When water levels equilibrate back toward the static level following a slug event, the observed water levels can be used to estimate a lower-bound value for transmissivity based on the rate of water level recovery. The following formula, in mixed units, can be applied to perform the calculation:

$$T = \frac{1.25}{t} \ln \frac{y_1}{y_2} \ln \frac{R}{r_w} \left(D^2 - d^2 \right),$$

where

T = transmissivity, in ft^2/day
y_1, y_2 = measurements of the water level change from static conditions, in feet
t = elapsed time between measurements, in minutes
R = effective radius of influence, in feet
r_w = borehole radius, in feet (0.51 feet)
D = inside diameter of well casing, in inches (4.5 inches)
d = outside diameter of drop pipe, in inches (1.315 inches)

Both the Hvorslev (1951) method and the Bouwer & Rice (1976) method were used to estimate the lower-bound transmissivity value. In the Hvorslev method, the value of *R*, the effective radius of influence, is chosen based on the well and aquifer geometry. For example, in a well screened at the bottom of a thick aquifer, *R* is set equal to twice the well screen length. In the Bouwer & Rice method, *R* is determined graphically using an empirical method developed by Bouwer & Rice.

Specific Capacity Method

The specific capacity of the pumped well can be used to obtain a lower-bound value of hydraulic conductivity. The hydraulic conductivity is computed using formulas that are based on the assumption that the pumped well is 100 percent efficient. The resulting hydraulic conductivity is the value required to sustain the observed specific capacity. If the actual well is less than 100 percent efficient, it follows that the actual hydraulic conductivity would have to be greater than calculated to compensate for well inefficiency. Thus, because the efficiency is unknown, the computed hydraulic conductivity value represents a lower bound. The actual conductivity is known to be greater than or equal to the computed value.

The Cooper-Jacob equation can be rearranged and iterated to solve for the lower-bound hydraulic transmissivity as follows:

$$T = \frac{264Q}{s} \log \frac{0.3Tt}{r_w^2 S},$$

where all terms are as defined above and r_w represents the radius of the borehole.

To apply this formula, a storage coefficient value must be assigned. The assigned value was based on unconfined conditions, based on the observation of delayed yield phenomena, signaling drainage of the sediments above the screened interval in the I-6 test. Storage coefficient values for unconfined aquifers typically range from a few percent to 20 percent or more, with the majority of the values falling between approximately 5 and 15 percent. Thus, in the absence of site-specific storage coefficient data, a value of 0.1 is deemed to be a reasonable choice for performing the calculations for unconfined conditions. The calculation result is not particularly sensitive to the choice of storage coefficient value, so a rough estimate of the storage coefficient is adequate to support the calculations. A storage coefficient value of 0.1 was applied to the calculations using late time data from the I-6 27-hour constant-rate pumping test. Some specific capacity based, lower-bound transmissivity estimates were made also from early data from the slug test response mentioned above following packer deflation. For these early time analyses, an elastic storage coefficient of 0.001 was used in the calculations. This magnitude of elastic storage is typical of early time response in unconfined systems.

Note that transmissivity appears on both sides of the equation as presented above. This means that an iterative solution must be used to obtain a solution.

Computing the lower-bound estimate of hydraulic conductivity can provide a useful frame of reference for evaluating the other pumping test calculations.

I-6 Data Analysis

This section presents the data obtained from the I-6 test pumping and the results of the analytical interpretations. Analyses were applied to the four trial pumping events and the 27-hour constant-rate pumping test.

Background Data

Figure 1 shows the apparent water level hydrograph for I-6 and the barometric pressure data recorded throughout the testing period. The graph shows that the barometric pressure fluctuations were minor, spanning just 0.2 feet. The vertical scale for the hydrograph is compressed, masking subtle groundwater pressure fluctuations, but the graph provides a sense of the water level responses during testing. Figure 2 shows a typical segment of the Figure 1 data, from late February 25 to early February 26 just before the start of the constant-rate test, with the vertical axes scaled the same for aquifer and barometric pressure. The groundwater pressure changes associated with ongoing water level recovery appeared to be unaffected by changes in barometric pressure. This implied a barometric efficiency of nearly 100 percent, consistent with the barometric efficiencies observed in most of the wells on the plateau.

The most significant observation was that, unlike the regional aquifer test results that showed rapid water level recovery back to static conditions, the perched zone water levels recovered sluggishly, falling short of the starting static water level after each pumping event. Note, however, that the apparent drop in head between the first pump installation on February 24/25 and the second pump installation on February 25/26 was exaggerated by an offset in the installation depth – the second installation was about one foot shallower. Nevertheless, the

decline in water level peaks was apparent, especially after the 27-hour constant-rate pumping test. This response suggested boundary conditions indicating a laterally limited saturated zone, rather than an areally extensive one.

Trial 1 Pumping Test

Trail 1 was conducted on February 24. The well was pumped at 1.83 gpm for 69 minutes from 3:14 pm to 4:23 pm. Following shutdown, recovery measurements were recorded for 120 minutes until 6:23 pm.

Time-Drawdown Analysis

Figure 3 shows time-drawdown data from trial 1. Because the pump started against an empty drop pipe, the low initial head resulted in a high initial discharge rate. As the drop pipe filled, the pumping rate declined.

The initial submergence of the transducer was 26.66 feet. Nevertheless, the recorded drawdown reached nearly 32 feet. This meant that a partial vacuum (about 5 feet) was created beneath the packer. It appeared, however, that the well remained reasonably well sealed and largely free from casing and filter pack storage effects. For example, the rapid initial drawdown (30 feet in less than two minutes) would not have been possible if significant casing or filter pack drainage had occurred.

However, as described below, there may have been a slow leak of vadose zone air into the filter pack when the well was drawn down. Such an occurrence would result in negligible storage response during pumping because of the low leakage rate, but once a small portion of the filter pack had drained during pumping, its presence would be obvious during recovery because the accumulated air at the top of the pack would compress like a spring when water levels rose following pump shut off.

The variable and unknown pumping rate precluded analysis of the drawdown data.

Recovery Analysis

Figure 4 shows a semilog plot of the recovery data following the trial 1 pumping. The transmissivity calculated form the graph was 48 gpd/ft. Note that the early recovery data did not fall on the straight line of best fit, implying that the *u* value was greater than 0.05 and that Theis curve matching should be used to solve for transmissivity.

Figure 5 shows Theis curve matching analysis of the data, revealing a transmissivity estimate of 60 gpd/ft. This is likely more accurate than the value obtained from the semilog plot.

Note on Figure 4 that at the end of the recovery, 0.4 feet of drawdown remained. This is strong evidence of a negative boundary. The negative boundary could be either a limit in the size of the saturated perched zone or, alternatively, a reduction in hydraulic conductivity some distance from the pumped well. The latter scenario is possible here, as perched zones are known to exist in both R-15 and I-5 at similar elevation, and the hydraulic conductivity of the I-5 sediments is very low.

About 30 minutes into recovery, water levels dropped 0.25 feet over a 10-minute period and then rebounded (the "wiggle" in the data curve at late recovery time on Figure 4). There was no explanation for this exceedingly unusual response. No other recovery data sets showed the effect.

An interesting feature of the plot on Figure 5 is the deviation from the type curve during the first minute of recovery. This has the appearance of a very small storage effect – perhaps just a fraction of a gallon total volume, based on the limited duration. A possible explanation could be minor antecedent drainage of a very small portion of the filter pack, allowing refilling during recovery. Because the hypothesized drained portion of the filter pack was 20 feet above the top of the screened interval, there would be a very short delay in observing its effect, consistent with the observations on Figure 5. The observed straight-line segment on the log-log plot during the first minute of recovery (from 0.3 to 0.9 minutes) also was consistent with a storage phenomenon. It is only conjecture that filter pack storage caused the anomaly seen on Figure 5, but it is a reasonable hypothesis.

It is significant that the late data showed a flat slope. This suggests drainage from above – likely delayed yield associated with unconfined conditions at the top of the saturated zone.

Trial 2 Pumping Test

Trial 2 was conducted on February 24 following the trial 1 recovery. The well was pumped at multiple flow rates, ending at and averaging 1.7 gpm for 117 minutes from 6:23 pm to 8:20 pm. Following shutdown, recovery measurements were recorded for 908 minutes until packer deflation at 11:28 am on February 25.

Time-Drawdown Analysis

Figure 6 shows time-drawdown data from trial 2. The multiple discharge rates precluded analysis of the data. Note also that the very early data showed evidence of a check valve leak. Antecedent drainage of a small portion of the drop pipe, through a leaky check valve or leaky coupling joints, would have allowed the pump to start against reduced head briefly, resulting in a momentary higher pumping rate and greater drawdown.

Recovery Analysis

Figure 7 shows the recovery data following the trial 2 pumping. The transmissivity calculated form the graph was 52 gpd/ft. Note that the early recovery data did not fall on the straight line of best fit, implying that the *u* value was greater than 0.05.

Figure 8 shows Theis curve matching analysis of the data, revealing a transmissivity estimate of 68 gpd/ft. This is likely more accurate than the value obtained from the semi log plot.

Note that the last measured water level was 0.5 feet below the static level even after recovering overnight. This provided additional evidence of the presence of a negative boundary.

The same very brief storage response observed in trial 1 was seen on Figure 8. Finally, the flat slope of the late data again suggested delayed yield associated with unconfined conditions.

Slug Event Caused By Packer Deflation

Following trial 2 recovery, it was discovered that the check valves had failed allowing drainage of the drop pipe. Therefore, the decision was made to remove the pump, replace the check valves and redo the trial tests. When the packer was deflated, the head above the transducer increased by more than 35 feet, indicating that a substantial volume of water had leaked from the drop pipe into the annulus above the packer. Deflating the packer allowed the trapped water to flow down the well and into the perched zone.

Figure 9 shows the hydraulic response measured following packer deflation. Data from this event were used to estimate a lower-bound transmissivity using the specific capacity method. This was done by observing the rate of drainage of the well casing for a given head buildup. From this it was possible to calculate a specific capacity to use in estimating transmissivity.

For example, between 1 and 1.1 minutes following packer deflation, 0.414 gallons of water drained into the aquifer with an average head buildup of 31.52 feet. This made the flow rate into the aquifer 4.14 gpm and the specific capacity 4.14/31.52 = 0.131 gpm/ft at an average injection time of 1.05 minutes. Assuming a storage coefficient value of 0.001 and applying the Cooper-Jacob equation yielded a lower-bound transmissivity estimate of 59 gpd/ft. Similarly, at 2.05 minutes of injection, the inflow rate was 3.23 gpm with 26.65 feet of head buildup, for a specific capacity of 0.121 gpm/ft. The corresponding lower bound transmissivity estimate was 65 gpd/ft. These values were consistent with the pumping test transmissivity estimates.

Trial 3 Pumping Test

Trial 3 was conducted on February 25. The well was pumped at 1.8 gpm for 20 minutes from 3:41 pm to 4:01 pm. Following shutdown, recovery measurements were recorded for 70 minutes until 5:11 pm.

Drawdown Analysis

Figure 10 shows time-drawdown data from trial 3. Because the pump started against an empty drop pipe, the low initial head resulted in a high initial discharge rate. As the drop pipe filled, the pumping rate declined.

The initial submergence of the transducer was 25.75 feet. Nevertheless, the recorded drawdown reached nearly 34 feet. This meant that a partial vacuum (about 8 feet) was created beneath the packer. Again, it appeared that the well remained reasonably well sealed and largely free from casing and filter pack storage effects. For example, the rapid initial drawdown (33 feet in less that two minutes) would not have been possible if significant casing or filter pack drainage had occurred.

Because of the variable pumping rate, the data were not analyzed.

Recovery Analysis

Figure 11 shows the recovery data following the trial 3 pumping. The transmissivity calculated from the graph was 49 gpd/ft. Again, the early recovery data did not fall on the straight line of best fit, implying that the *u* value was greater than 0.05.

Figure 12 shows Theis curve matching analysis of the data, revealing a transmissivity estimate of 64 gpd/ft. This is likely more accurate than the value obtained from the semilog plot.

As in previous recovery plots, the data showed the momentary storage effect (Figure 12) and sustained drawdown (0.75 feet) at the end of recovery (Figure 11), confirming the negative boundary.

Trial 4 Pumping Test

Trial 4 was conducted on February 25 following the trial 3 recovery. The well was pumped at 1.84 gpm for 71 minutes from 5:11 pm to 6:22 pm. Following shutdown, recovery measurements were recorded for 848 minutes until 8:30 am on February 26.

Time-Drawdown Analysis

Figure 13 shows time-drawdown data from trial 4. The Cooper-Jacob analysis yielded a transmissivity of 62 gpd/ft. Figure 14 shows the results of the Theis analysis yielding a transmissivity value of 60 gpd/ft. There was negligible apparent storage response in the data as would be expected if a slow leak had been the cause of the eventual storage responses observed in the recovery data. Finally, the effects of delayed yield were apparent in the flattening of the data curve at late time.

Recovery Analysis

Figure 15 shows the recovery data following the trial 4 pumping. The transmissivity calculated form the graph was 51 gpd/ft. As in the other trial tests, the early recovery data did not fall on the straight line of best fit, implying that the u value was greater than 0.05.

Figure 16 shows Theis curve matching analysis of the data, revealing a transmissivity estimate of 68 gpd/ft. This is likely more accurate than the value obtained from the semilog plot.

Both the momentary storage effect and the late flat slope associated with delayed yield from above were apparent in the data plots on Figures 15 and 16. The final water level remained 0.75 feet below the starting level, even after nearly a day of recovery, consistent with negative boundary conditions.

27-Hour Constant-Rate Pumping Test

The 24-hour constant-rate pumping test was begun at 8:30 am on February 26. The well was pumped at 1.94 gpm for 1620 minutes until 11:30 am the next day. Following shutdown, recovery measurements were recorded for 1266 minutes until 8:36 am on February 28.

Time-Drawdown Data

Figures 17 and 18 show semilog and log-log plots of time-drawdown data from the 27-hour constant-rate pumping test. Note that the recorded time values were adjusted by an offset of 0.8 seconds before plotting to account for the elapsed time between the last background water level measurement and pump startup. (The offset value was determined by adjusting it until the Theis type curve provided a good match to the data.)

The calculated transmissivity values from the early data were 74 gpd/ft and 65 gpd/ft from the two graphs. Note that there was no evidence of a storage response in the early drawdown data, consistent with what was observed in the trial 4 draw-down data.

The data showed the flattening associated with delayed yield, similar to the trial tests. In addition, the test was long enough to show the resumption of a steep slope at late time, once drainage associated with delayed yield was complete. Figure 19 shows an expanded-scale graph of the late data from which a transmissivity of 68 gpd/ft was calculated. Although this value agreed with other results, this was probably fortuitous and not an independent measurement of transmissivity. The late data would be expected to reflect the entire transmissivity of the saturated zone – both the screened portion and the interval above the well screen. Thus, the late-time slope should have been flatter, yielding a greater transmissivity. It is likely that the slope was affected by the suspected boundary conditions and that the compensating factors of increased transmissivity (of the entire saturated thickness) and the negative boundary resulted in a slope that was coincidentally similar to the early-time slope.

The Neuman method for unconfined aquifers was applied to the data, as shown on Figure 20. The resulting hydraulic conductivity value of 8 gpd/ft^2 was consistent with previous results. Multiplying this value by the effective screened interflow thickness of 8 feet yielded a transmissivity of 64 gpd/ft, consistent with other results. Note that at late time, the Neuman type curve predicted a flatter slope than that of the actual data trace. This confirmed the idea that the late time slope was affected simultaneously by both the transmissivity of the entire saturated thickness and boundary conditions.

Unusual transient drawdown fluctuations were seen in the late drawdown data. They showed up most clearly on Figure 17 as water level "spikes". The expanded-scale plot on Figure 21 shows these anomalies more prominently.

Pumping rate measurements showed that during the first peak there had been no change in discharge rate from the well to account for the temporary drawdown reduction. A possible explanation for this response was that the pumping water level in the aquifer was pulled low enough to relieve a portion of the partial vacuum in the borehole above the well screen, allowing drainage of an aquifer feature such as a fracture. For example, a submerged fracture filled with water would be under a vacuum and remain filled but, once exposed to vadose zone air, could possibly drain. The magnitude and duration of the water level peak were consistent with an influx of just a few gallons of water, so a minor aquifer feature could have accounted for the unusual response. While the actual cause of this anomaly was not completely clear, it was *not* attributable to a discharge rate fluctuation.

During the second peak, on the other hand, the discharge rate declined by two to three percent for a little less than 30 minutes, based on flow rate measurements made during the test. The drawdown response observed on the graph was consistent with this and, thus, resulted directly from the change in discharge rate. The mystery, however, is what caused the rate reduction. There was no apparent explanation for the observed change in production rate.

Recovery Analysis

Figure 22 shows a graph of the recovery data following the 27-hour constant-rate pumping test. The data are unusual in two respects. First, the storage response was more pronounced than those observed in the short trial tests. It is reasonable to assume that the extended pumping time allowed more filter pack or aquifer drainage to occur, thus creating a larger storage effect in the recovery data set. Second, there appeared to be a secondary storage effect in the data set. This phenomenon may be related to the refilling of previously drained aquifer features, such as fractures. Overall, the recovery data trace was much more "lumpy" than typical recovery graphs. This was ironic because, in most tests, the recovery curve is smoother and easier to analyze than the drawdown curve. In this test, however, the drawdown curve was more usable.

To illustrate the more pronounced storage response in the recovery data, Figure 23 provides a comparison of the recovery from the 27-hour test to recovery from trials 3 and 4. (All data were corrected mathematically to the same pumping rate for comparison purposes.) The trial test recovery curves were similar, deviating only slightly from the Theis type curve, as was shown on earlier plots. The 27-hour test recovery curve, on the other hand, showed a significant departure. Theoretically, all three curves should coincide.

Figure 24 shows another revealing comparison. The recovery data were converted to "calculated recovery" by extrapolating the original drawdown curve and computing the difference between the extrapolated drawdown and the residual drawdown. The calculated recovery data were plotted on the same graph as the original drawdown data. Theoretically, the two curves should coincide. Clearly, however, the drawdown trace showed no storage effect, while the calculated recovery curve showed significant storage effects. Note that after about 40 minutes the two curves did nearly coincide.

A final observation (Figure 22) was that after recovery overnight, the water level remained 1.74 feet below the static water level, or about 1 foot lower than the recovered level following trial 4. This reinforced the idea of significant boundary conditions.

Slug Event Caused By Packer Deflation

When the packer was deflated at the conclusion of testing, the head in the well rose more than 66 feet, similar to the response observed following the first packer deflation event. Figure 25 shows the measured hydraulic response. The early water level decay data were used to estimate lower-bound transmissivity values as was done previously.

The data showed a flow rate (casing drainage rate) into the aquifer of 6.63 gpm with 60.83 feet of head buildup after 1.05 minutes of flow. This information yielded a lower-bound transmissivity value of 46 gpd/ft. One minute later, the data showed an injection rate of 5.32

gpm with 52.93 feet of head buildup after 2.05 minutes, yielding a lower-bound transmissivity of 51 gpd/ft.

The overall data response was evaluated using both the Hvorslev method and the Bouwer & Rice method as shown in Figure 26. These analyses yielded lower-bound transmissivity values of 73 gpd/ft and 42 gpd/ft, respectively. It should be pointed out that the Hvorslev procedure is based on steady state pumping (i.e., long-term) and, as a result, overestimates the effective radius of influence, which, in turn, leads to an overestimate of transmissivity. This idea helps explain the high value of 73 gpd/ft obtained from this method.

Overall Average Hydraulic Properties

The drawdown and recovery analyses using Theis curve matching yielded transmissivity values ranging from 60 to 68 gpd/ft and averaging 64 gpd/ft. Assuming an 8-foot-thick interflow interval made the hydraulic conductivity 8.0 gpd/ft^2, or about 1.1 feet per day. The Neuman unconfined analysis yielded nearly identical values.

Specific Capacity Data

The observed specific capacity from I-6 was used to estimate lower-bound transmissivity values for the production zone for comparison to values obtained using conventional analysis techniques. After 27 hours of pumping the well at 1.94 gpm, the observed drawdown was 24.54 feet. Other input values used in the calculation included a storage coefficient of 0.1 and a borehole radius of 0.51 feet. The resulting lower-bound transmissivity value obtained using the Cooper-Jacob equation was 60 gpd/ft.

As discussed above, short-term specific capacity data from the slug events following packer deflation led to computed lower-bound transmissivity values ranging from 46 to 65 gpd/ft. Finally, the slug test analyses gave lower-bound values of 42 and 73 gpd/ft (with the latter value known to be the least realistic estimate).

In general, these results were consistent with the conventional test analyses.

Summary

The following information summarizes the results of the pumping and recovery tests on I-6:

1. Four short-duration trial tests and one 27-hour constant-rate pumping test were conducted on I-6.
2. The lack of clear response of formation pressure (apparent hydrograph) to changes in barometric pressure implied a barometric efficiency of nearly 100 percent, consistent with what has been observed in most of the wells on the plateau.
3. Casing storage effects were eliminated from the drawdown data sets. However, it appeared that a slow drainage event must have occurred during pumping, because the water level rebound following pump shutoff was storage-affected. The effect was slight in the short tests, but significant in the 27-hour test.

4. The transmissivity values calculated for the 8-foot-thick interflow zone were consistent, falling within a narrow range and averaging 64 gpd/ft. The resulting average hydraulic conductivity was 8.0 gpd/ft^2, or 1.1 feet per day.
5. Lower-bound transmissivity values obtained from specific capacity data and slug test responses averaged 57 gpd/ft, consistent with the transmissivity values obtained by conventional analysis.
6. The data showed the effects of delayed yield associated with unconfined conditions.
7. Water levels consistently failed to recover to the starting static water level after each pumping event, indicating negative boundary conditions, that is, a lateral limit to the perched zone or a permeability reduction away from the well (or both). The latter scenario is likely, because perched conditions are known to extend to R-15 and I-5 and the sediments in the I-5 perched zone are very tight.
8. The 27-hour pumping test showed unusual drainage-related responses that were probably related to saturated zone heterogeneities. It was possible that the drainage and refilling of discrete fractures or pockets of sediment caused the observed drawdown and recovery anomalies.

References

Bouwer, H. and R.C. Rice, 1976. "A Slug Test for Determining Hydraulic Conductivity of Unconfined Aquifers With Completely or Partially Penetrating Wells," Water Resources Research, vol. 12, no. 3, pp. 423-428.

Cooper, H.H., Jr. and C.E. Jacob, 1946. "A Generalized Graphic Method for Evaluating Formation Constants and Summarizing Well Field History," Transactions Am. Geophys. Union, vol. 27, no. 4, pp. 526-534.

Hvorslev, M.J., 1951. "Time Lag and Soil Permeability in Ground Water Observations," US Army Corps of Engineers Waterways Experimentation Station, Bulletin 36, 50 pp.

Neuman, S.P., 1974. "Effect of Partial Penetration on Flow in Unconfined Aquifers Considering Delayed Gravity Response," Water Resources Research, vol. 10, no. 2, pp. 303-312.

Schafer, D.C., 1978. "Casing Storage Can Affect Pumping Test Data," Johnson Drillers' Journal, Jan/Feb, Johnson Division, UOP Inc., St. Paul, Minnesota.

Theis, C.V., 1935. "The Relation Between the Lowering of the Piezometric Surface and the Rate and Duration of Discharge of a Well Using Groundwater Storage," Transactions Am. Geophys. Union, vol. 16, pp. 519-524.

Figure 1. Comparison of I-6 Apparent Hydrograph and TA-54 Adjusted Barometric Pressure

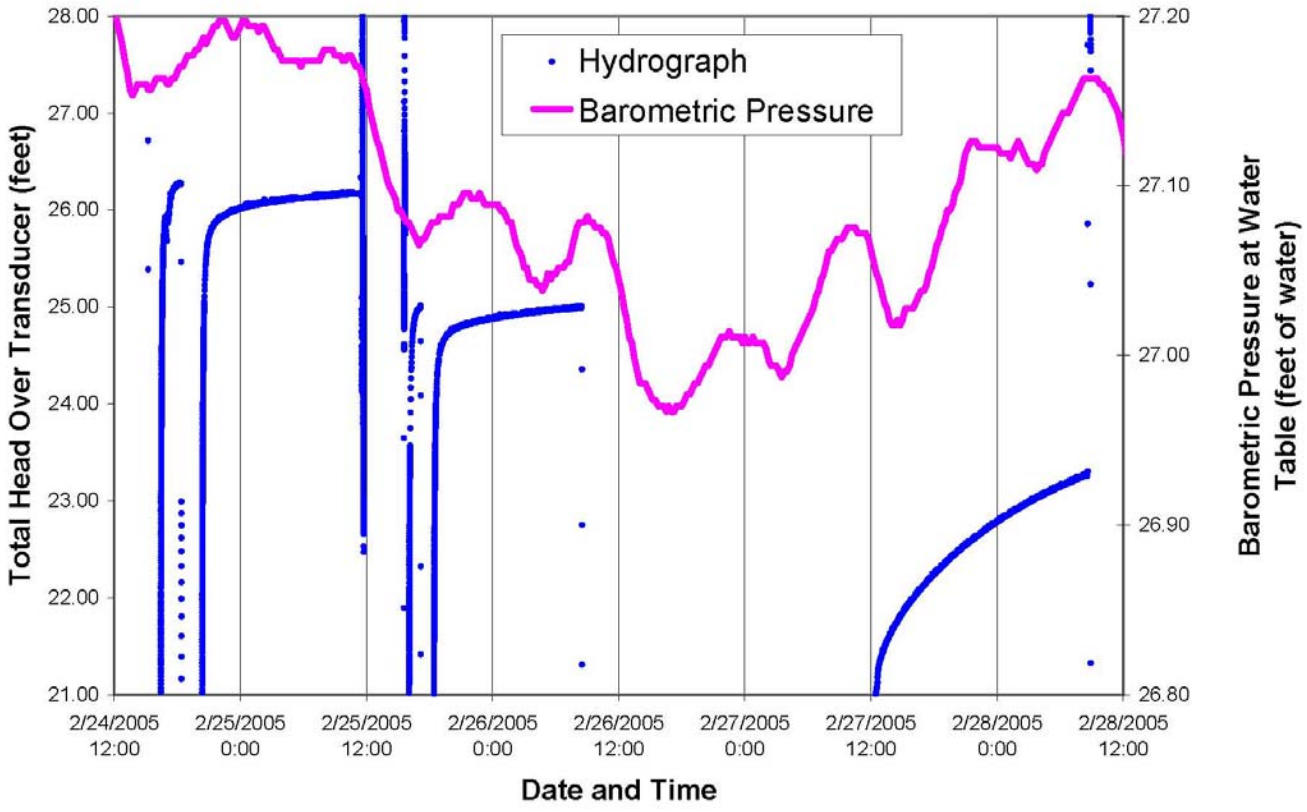

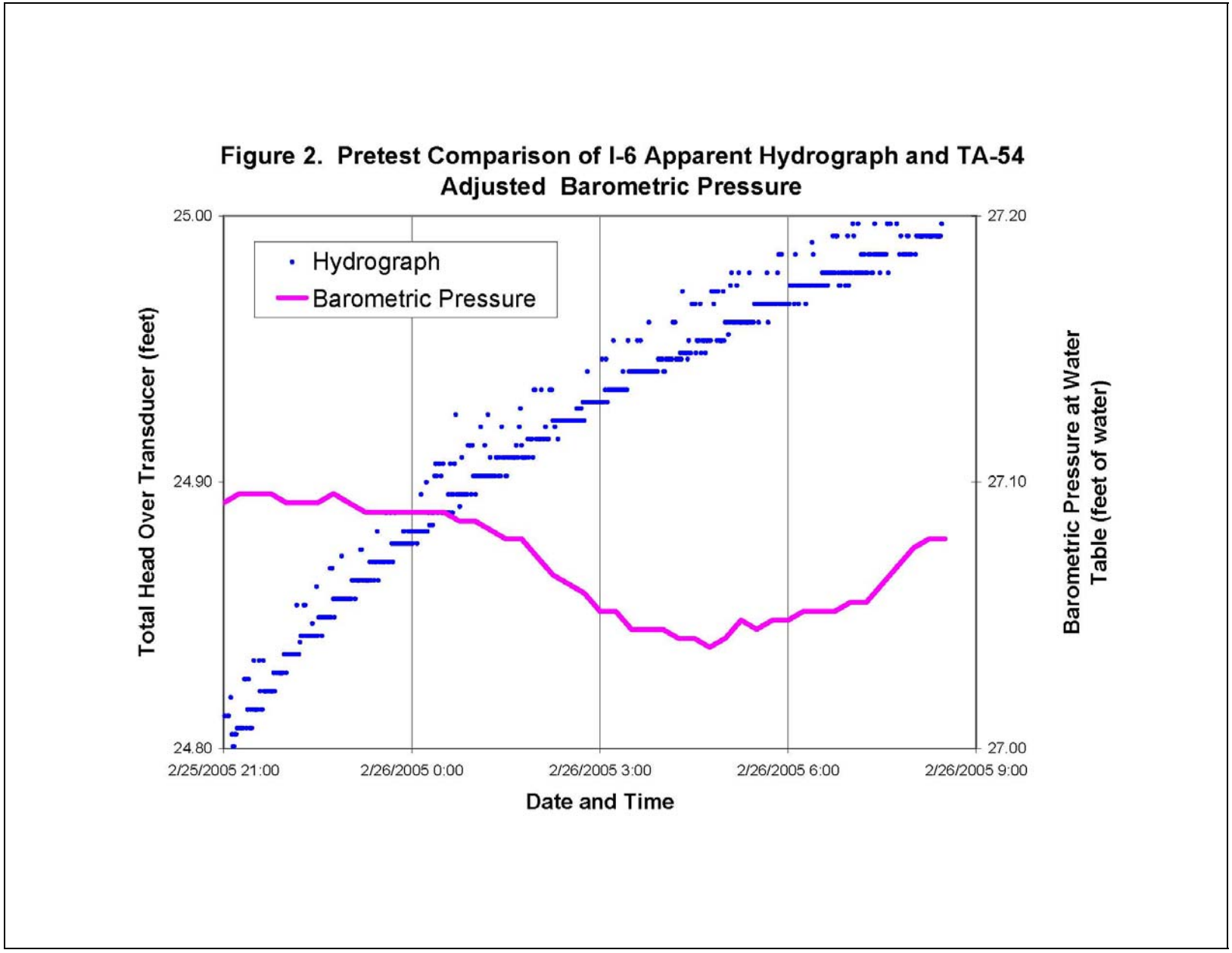
Figure 2. Pretest Comparison of I-6 Apparent Hydrograph and TA-54 Adjusted Barometric Pressure
Hydrograph
Barometric Pressure
Total Head Over Transducer (feet)
Barometric Pressure at Water Table (feet of water)
25.00
24.90
24.80
27.20
27.10
27.00
2/25/2005 21:00
2/26/2005 0:00
2/26/2005 3:00
2/26/2005 6:00
2/26/2005 9:00
Date and Time

Figure 3. Well I-6 Trial 1 Drawdown

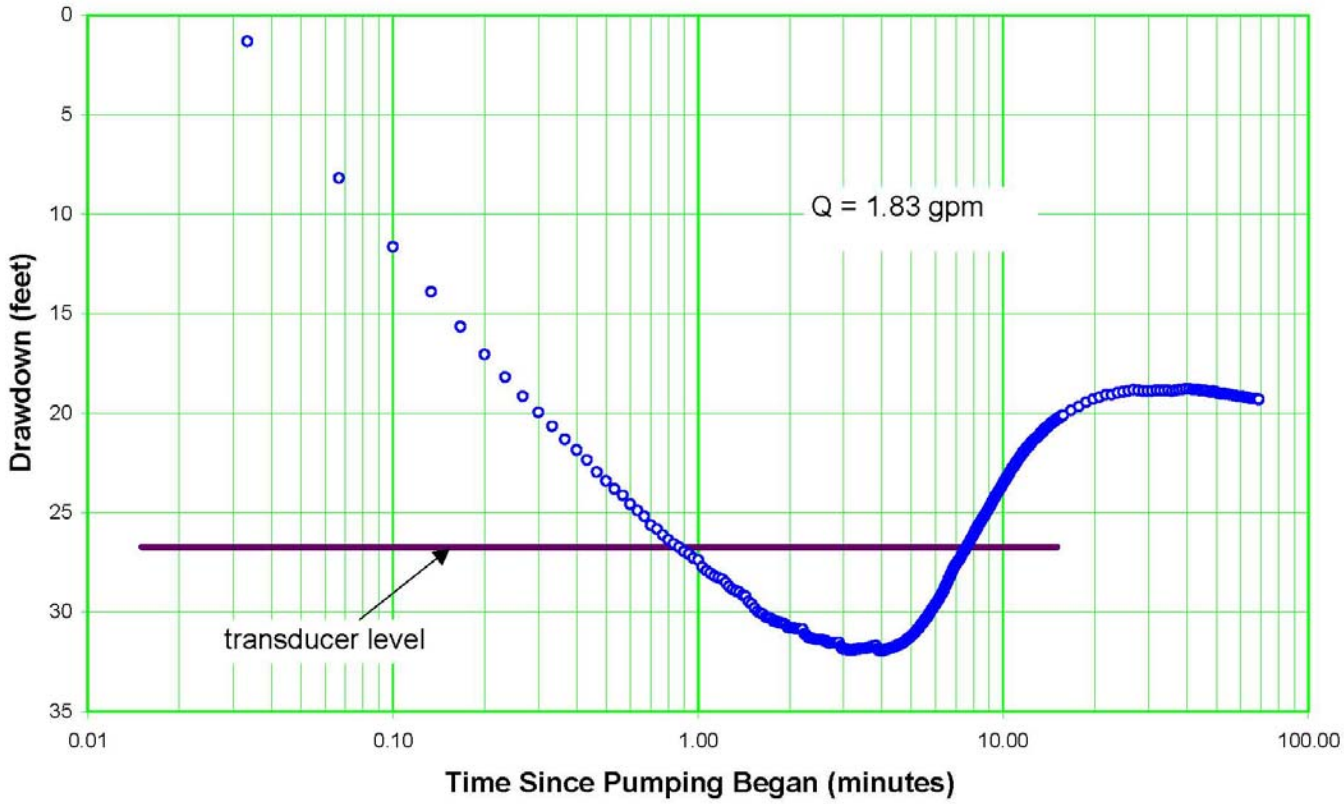

Figure 4. Well I-6 Trial 1 Recovery

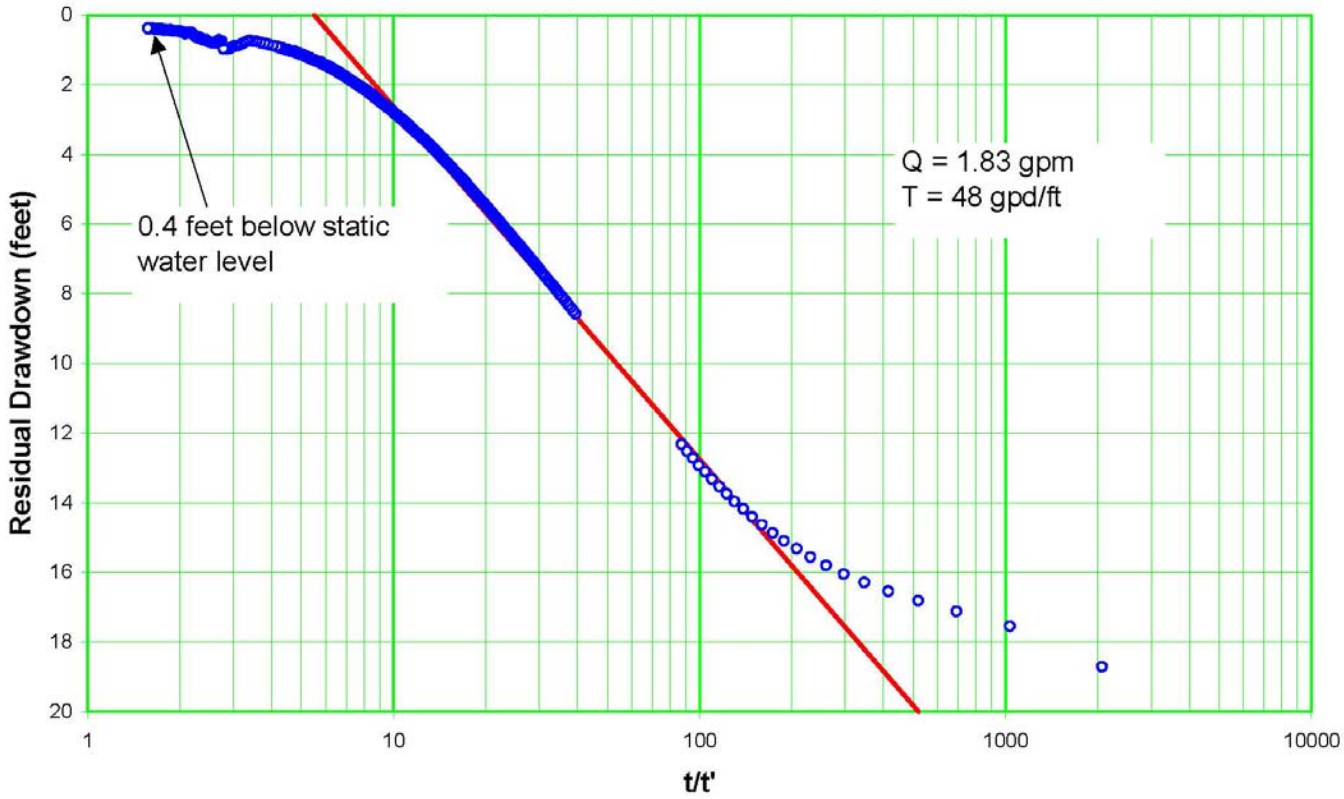

Figure 5. Well I-6 Trial 1 Recovery - Theis Analysis

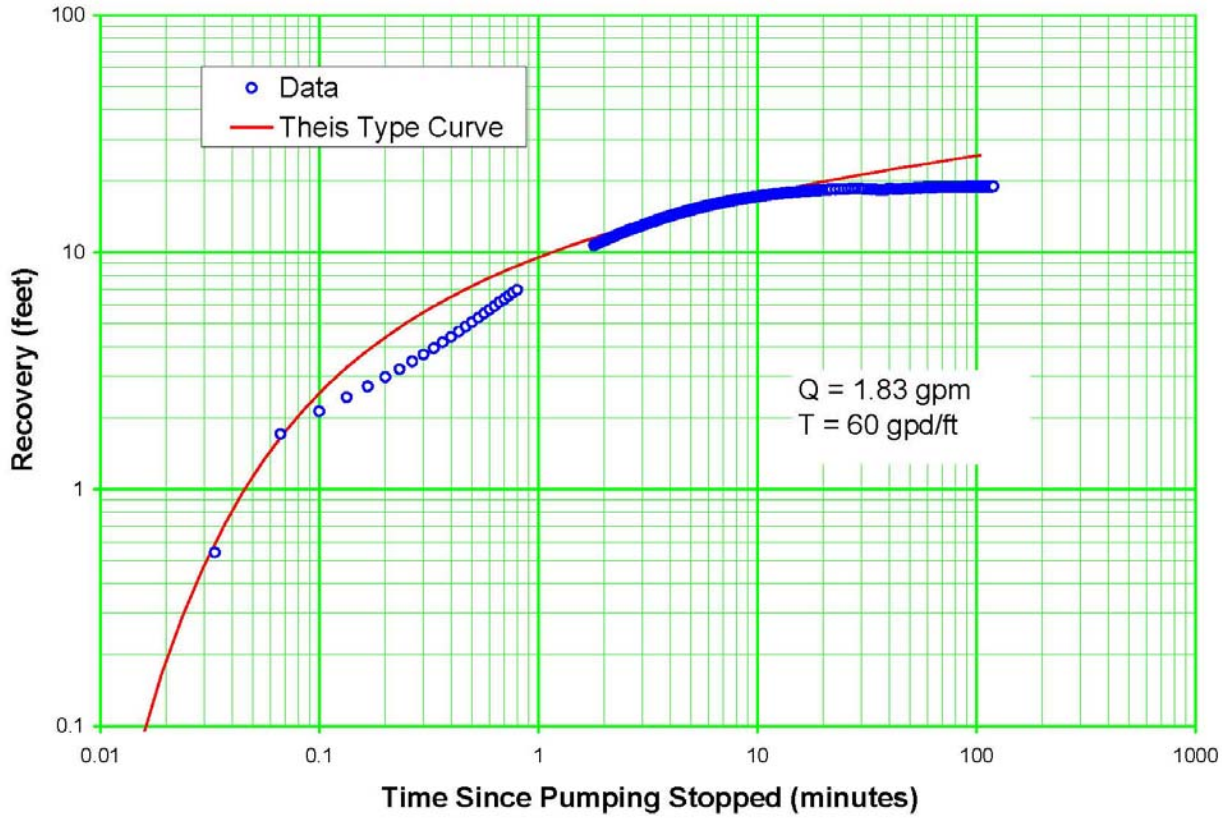

Figure 6. Well I-6 Trial 2 Drawdown

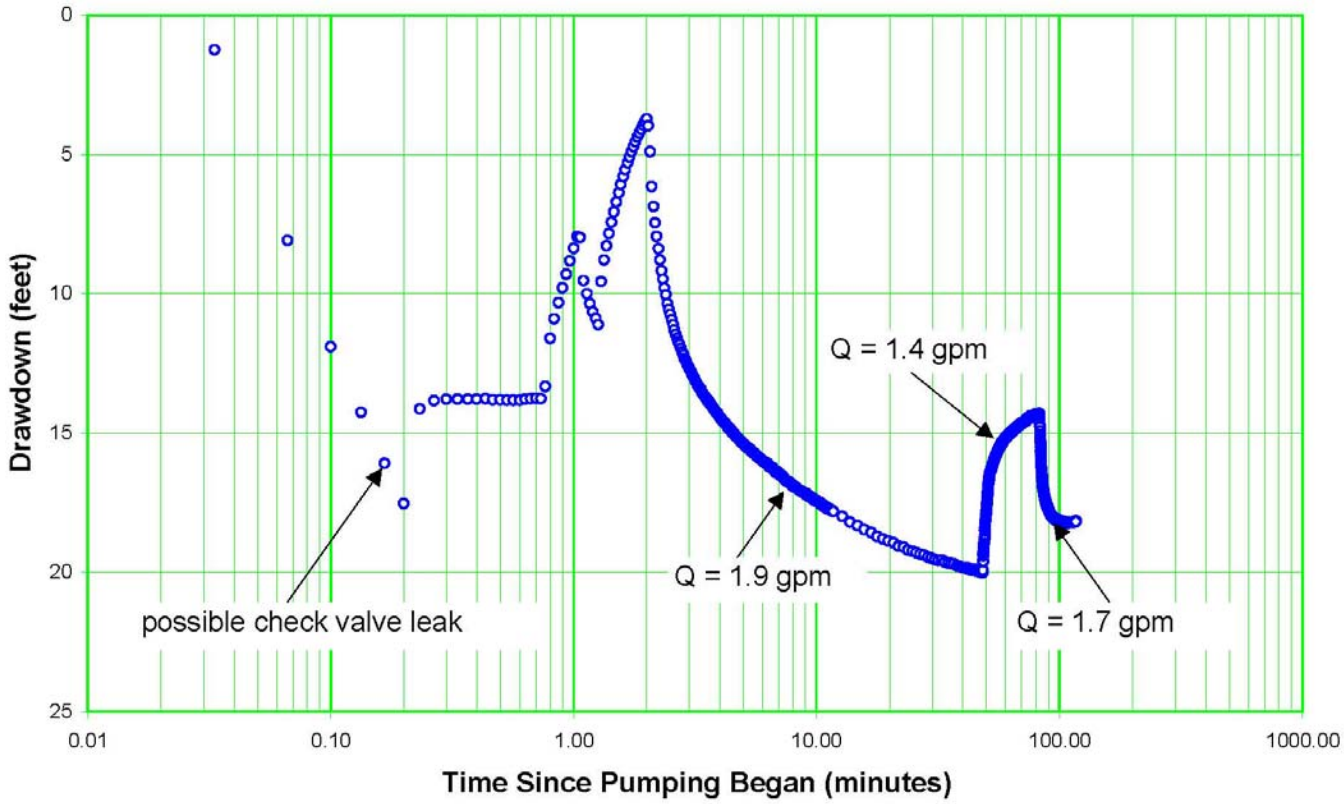

Figure 7. Well I-6 Trial 2 Recovery

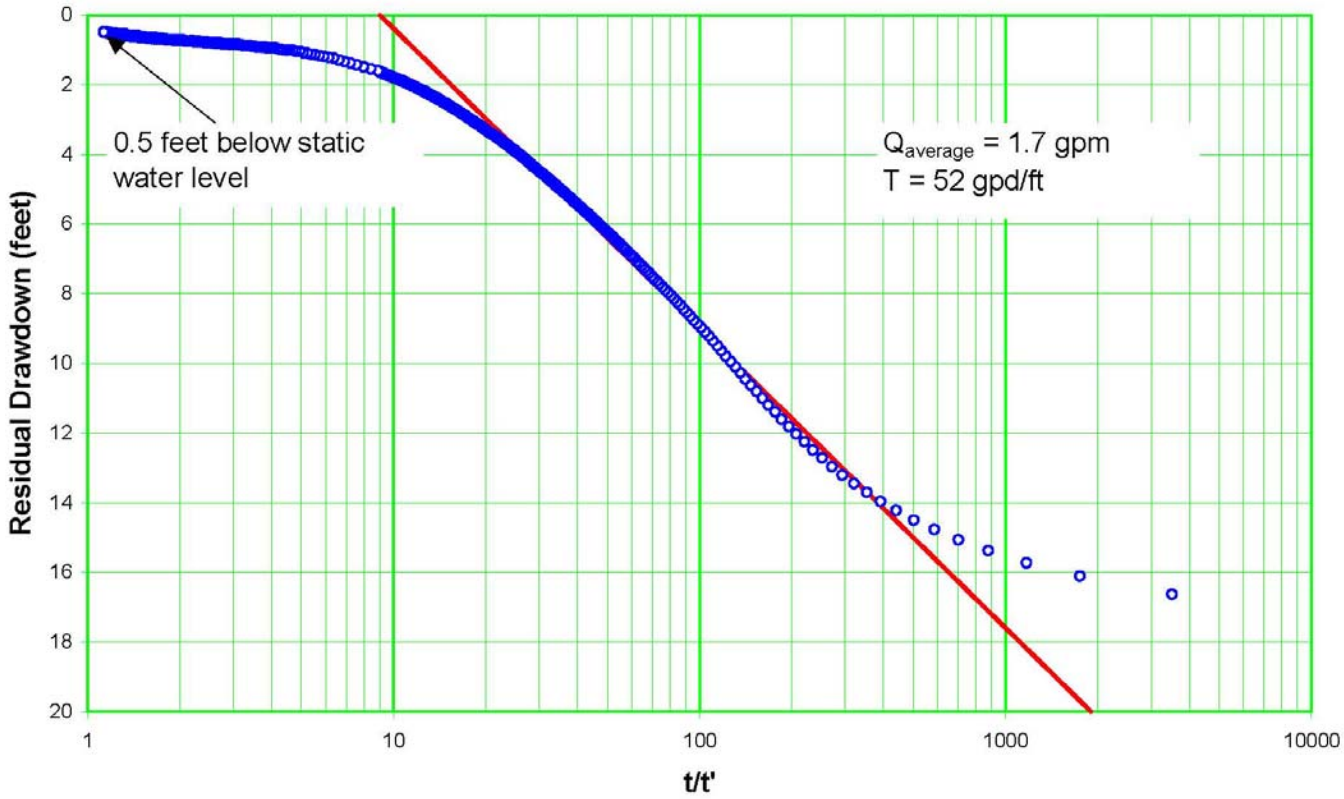

Figure 8. Well I-6 Trial 2 Recovery - Theis Analysis

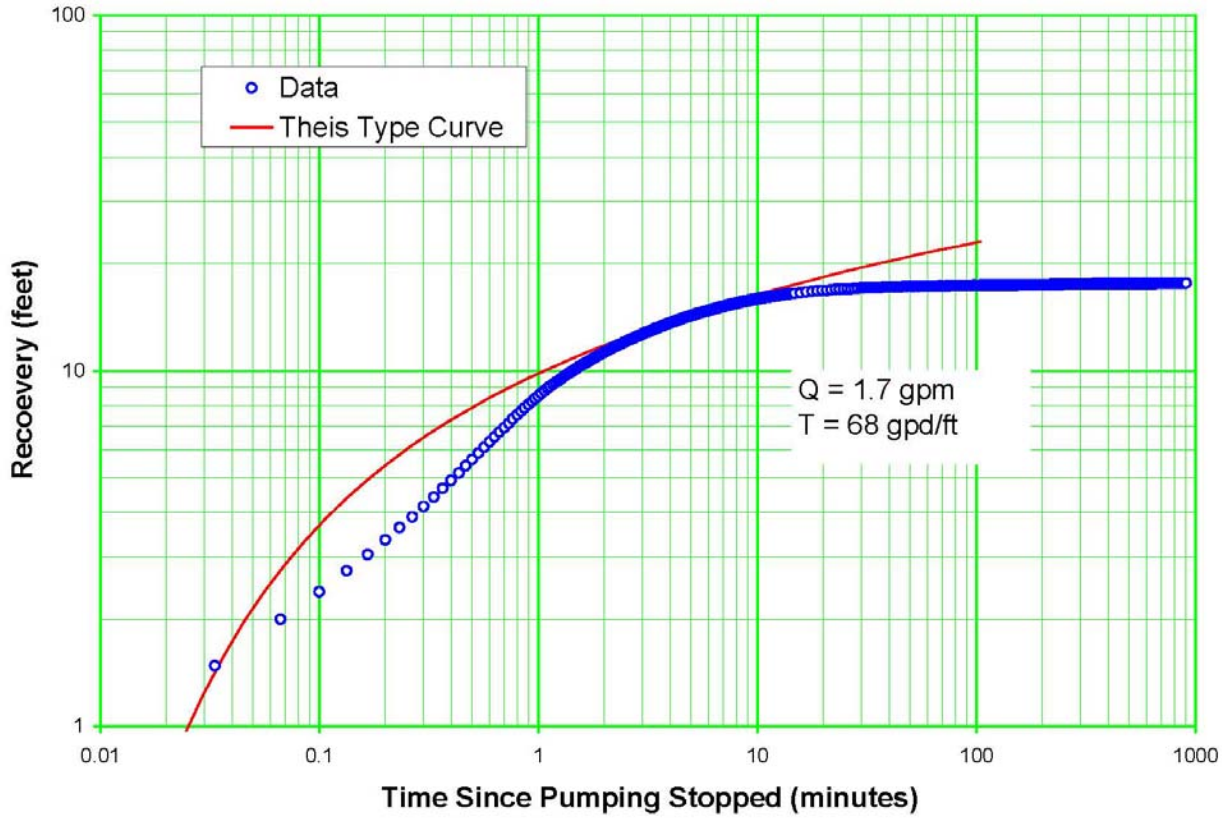

Figure 9. Packer Deflation Following Trial 2 Recovery

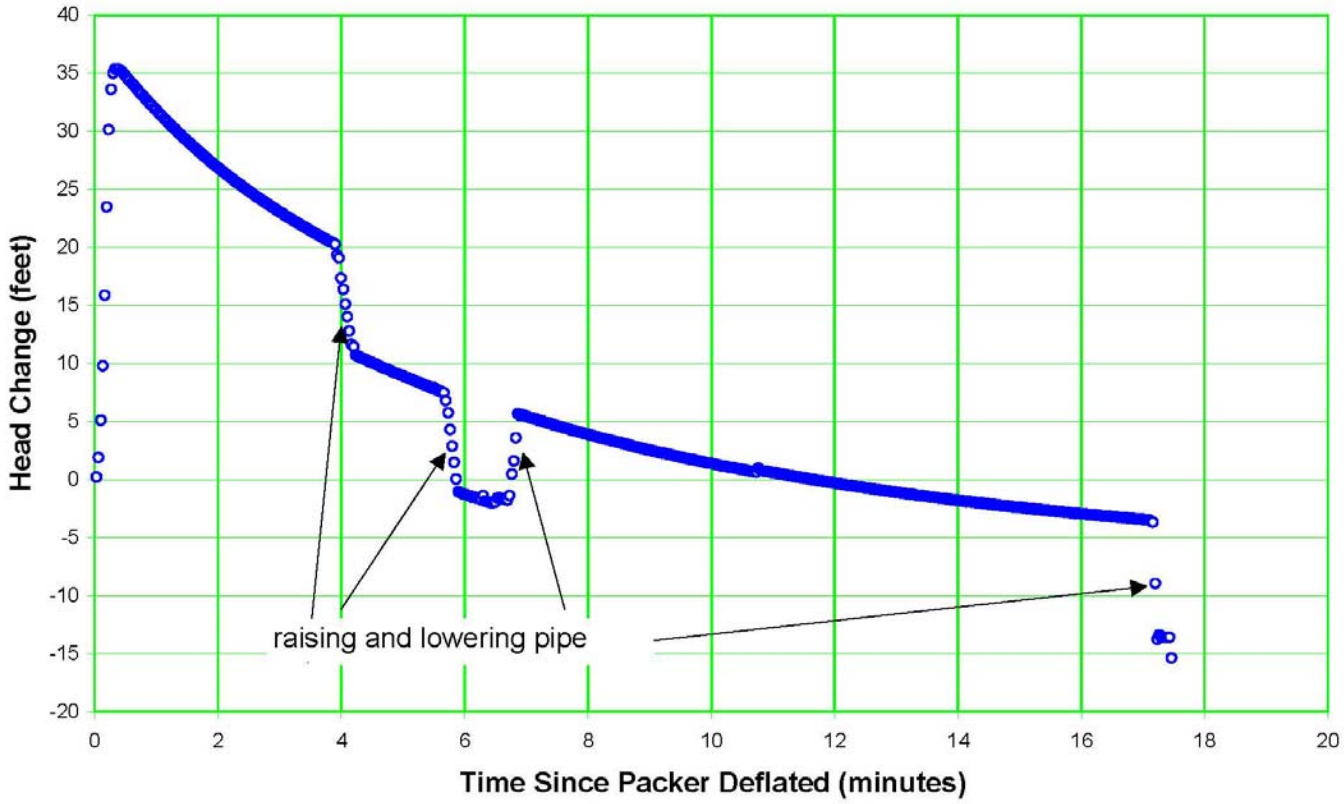

Figure 10. Well I-6 Trial 3 Drawdown

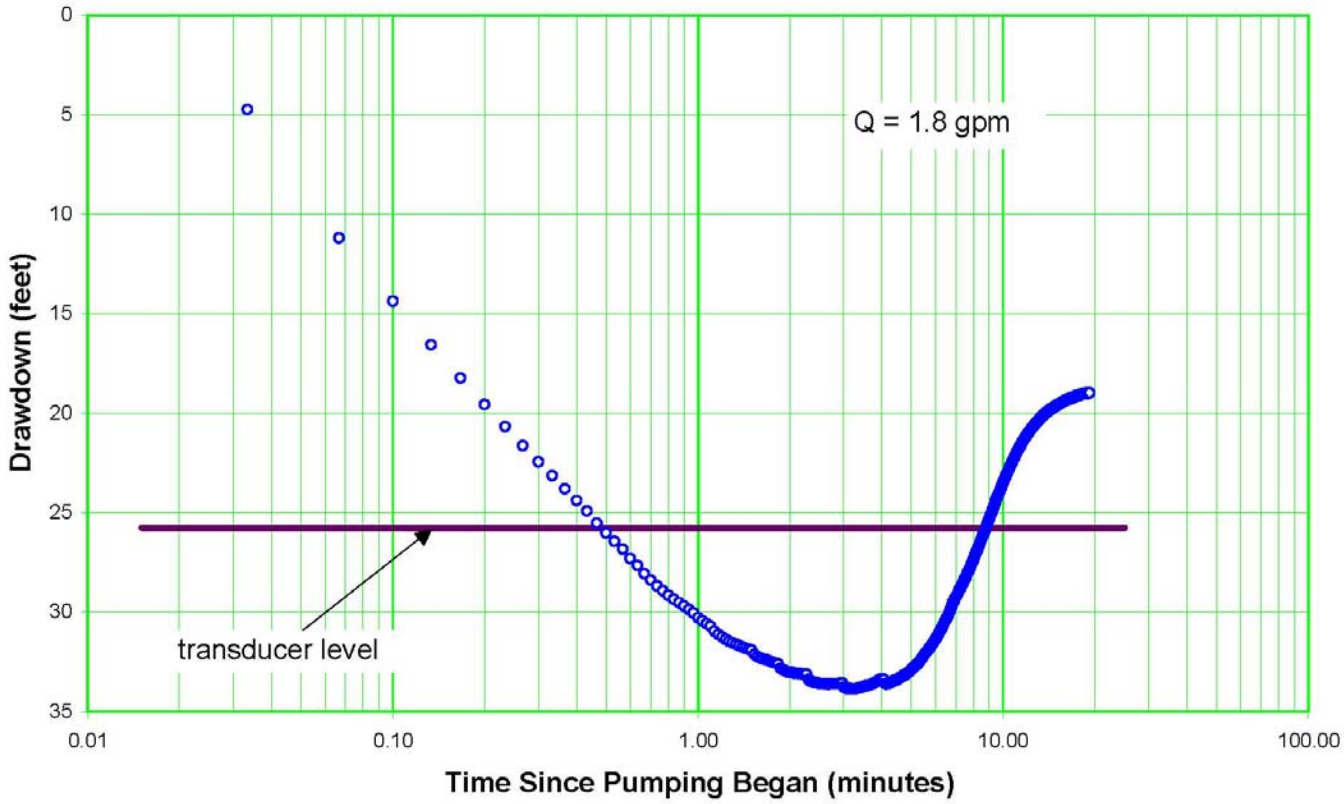

Figure 11. Well I-6 Trial 3 Recovery

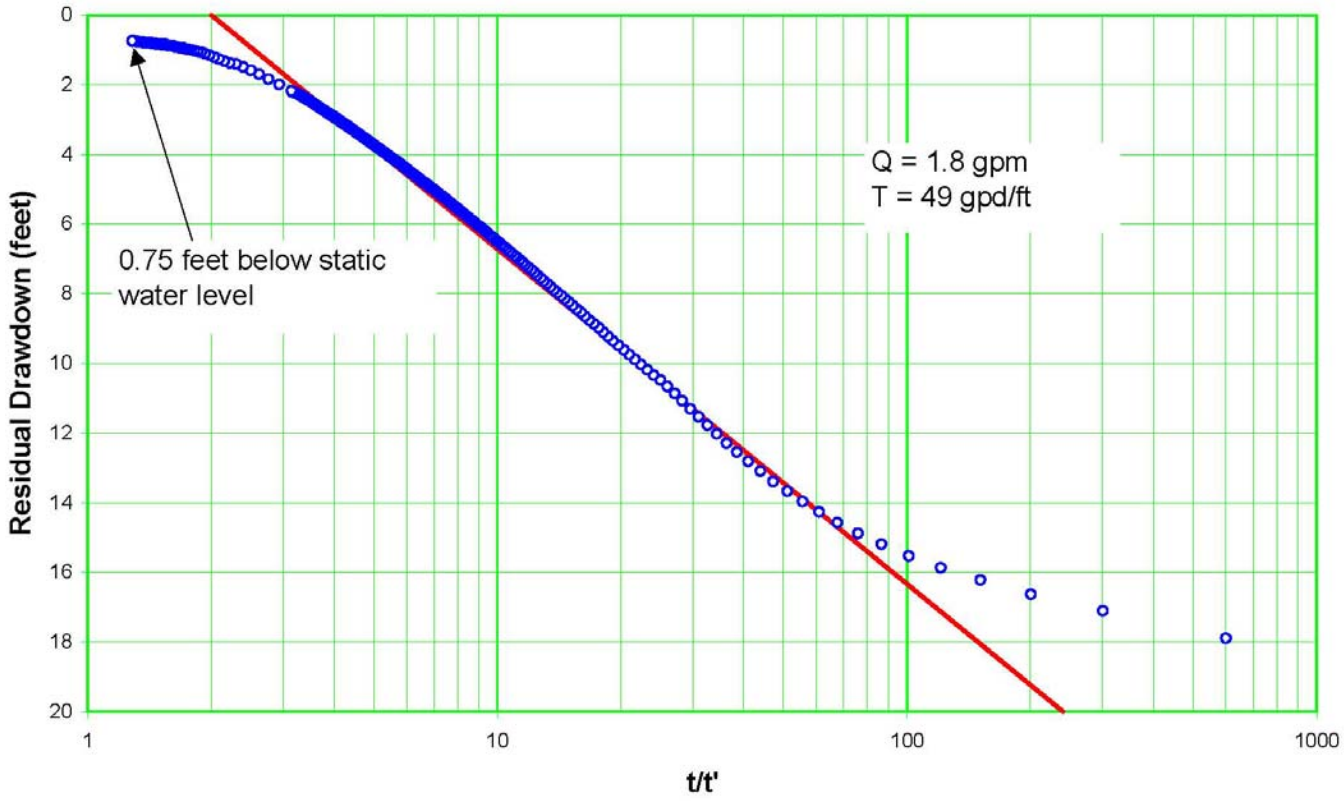

Figure 12. Well I-6 Trial 3 Recovery - Theis Analysis

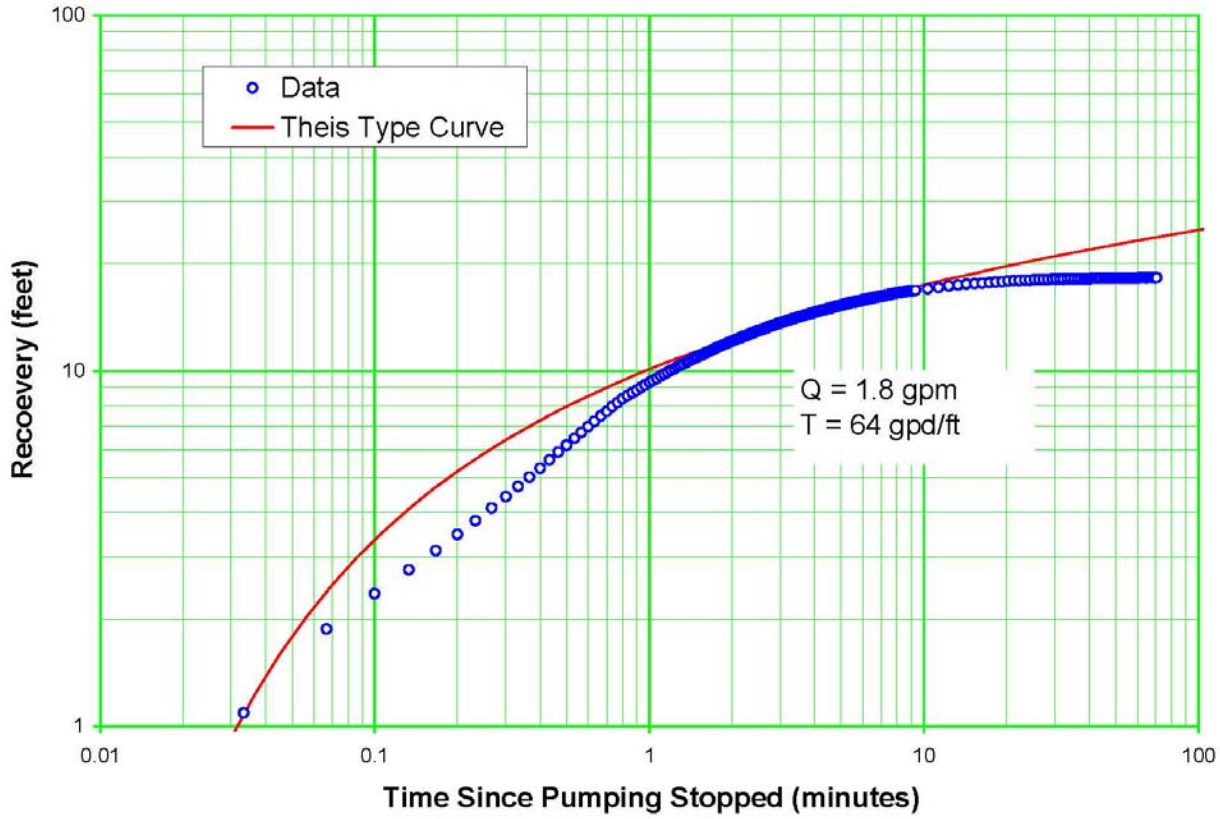

Figure 13. Well I-6 Trial 4 Drawdown

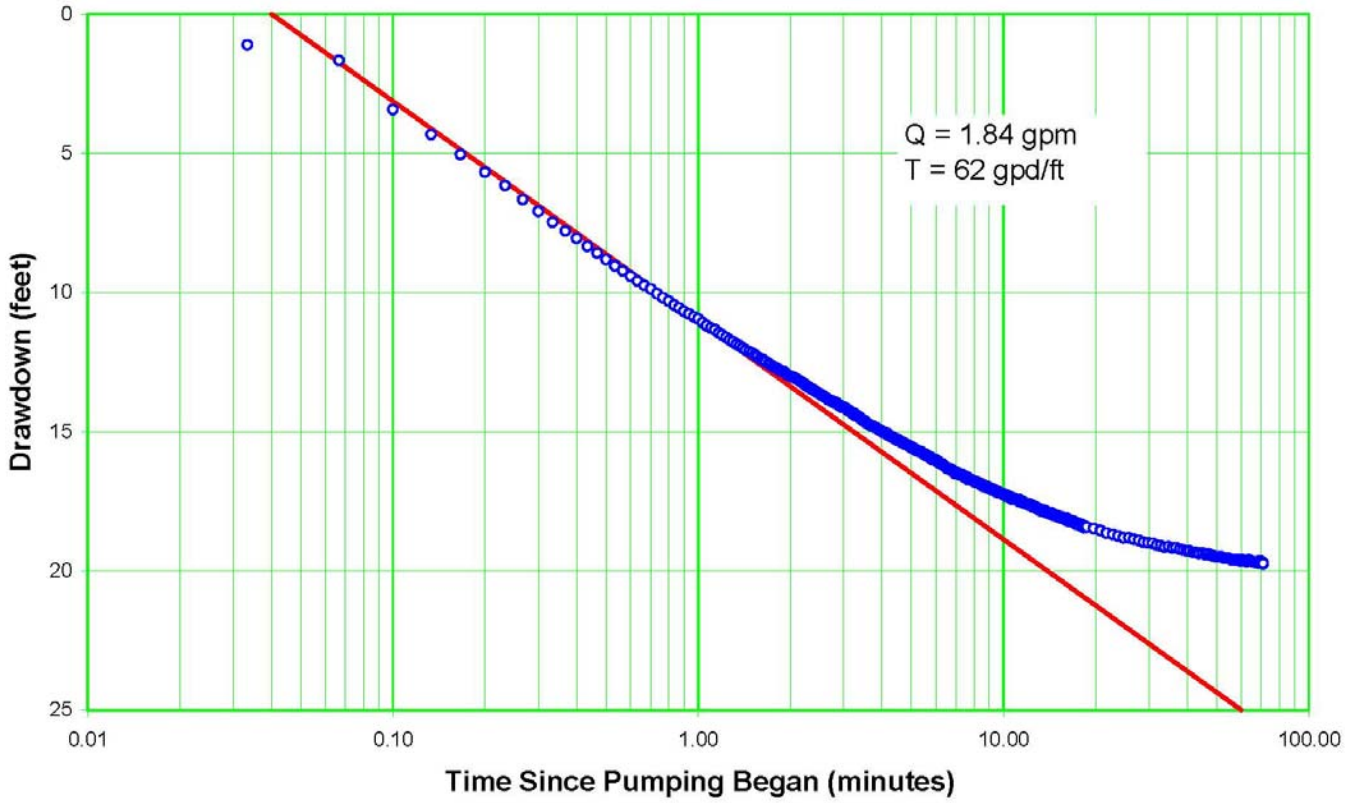

Figure 14. Well I-6 Trial 4 Drawdown - Theis Analysis

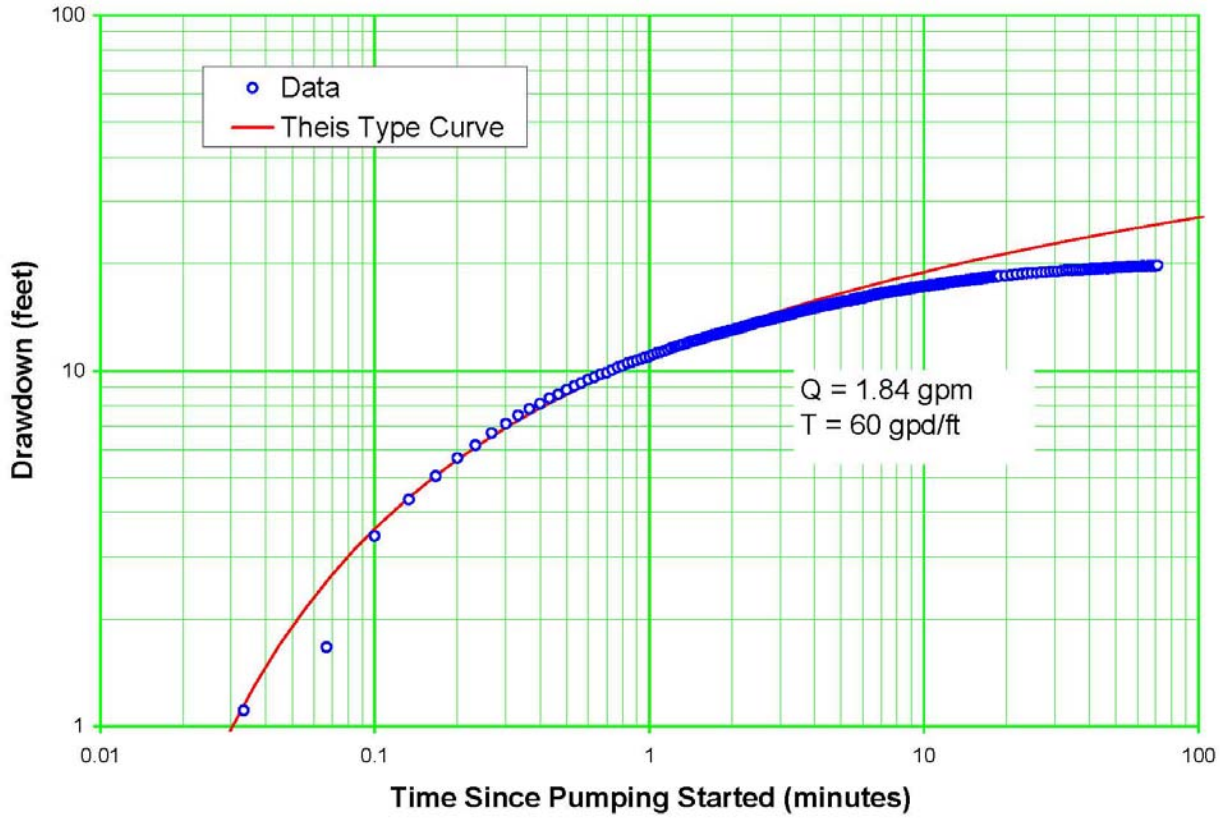

Figure 15. Well I-6 Trial 4 Recovery

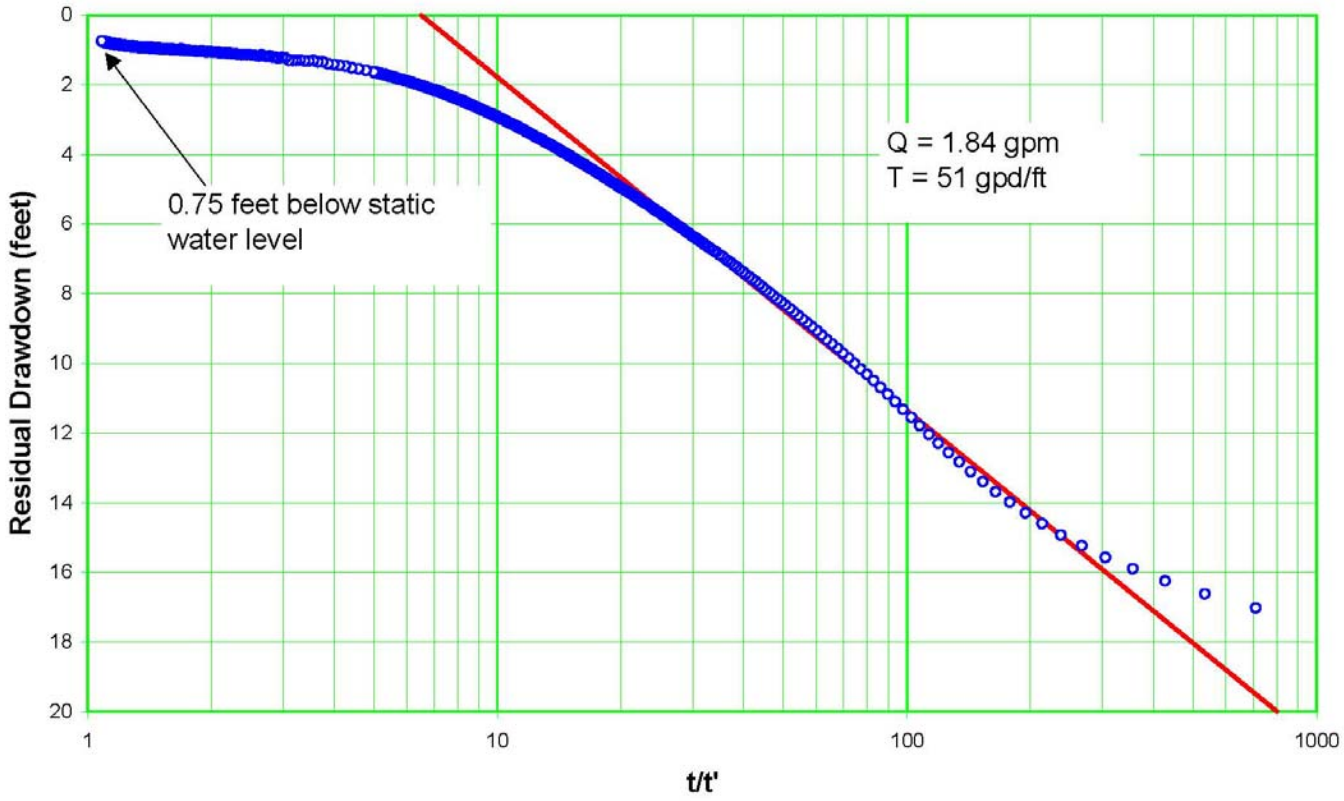

Figure 16. Well I-6 Trial 4 Recovery - Theis Analysis

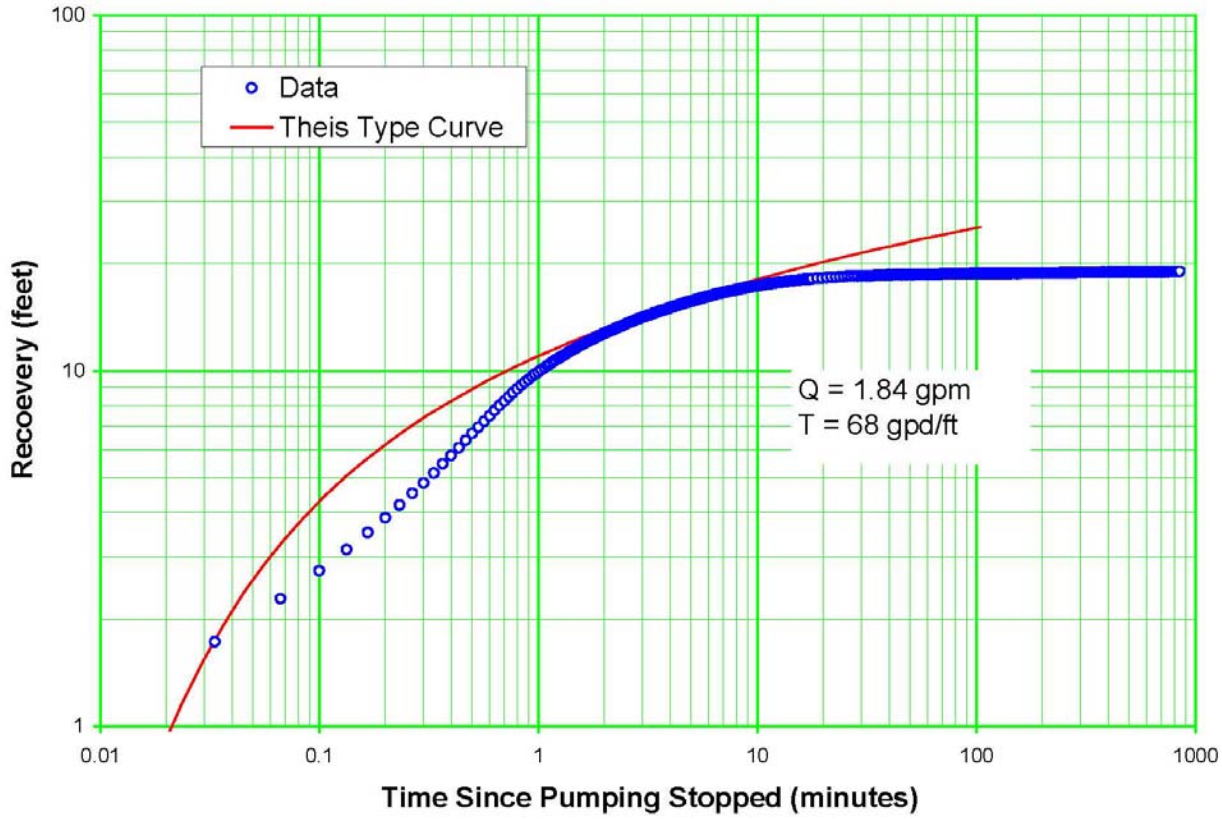

Figure 17. Well I-6 Drawdown

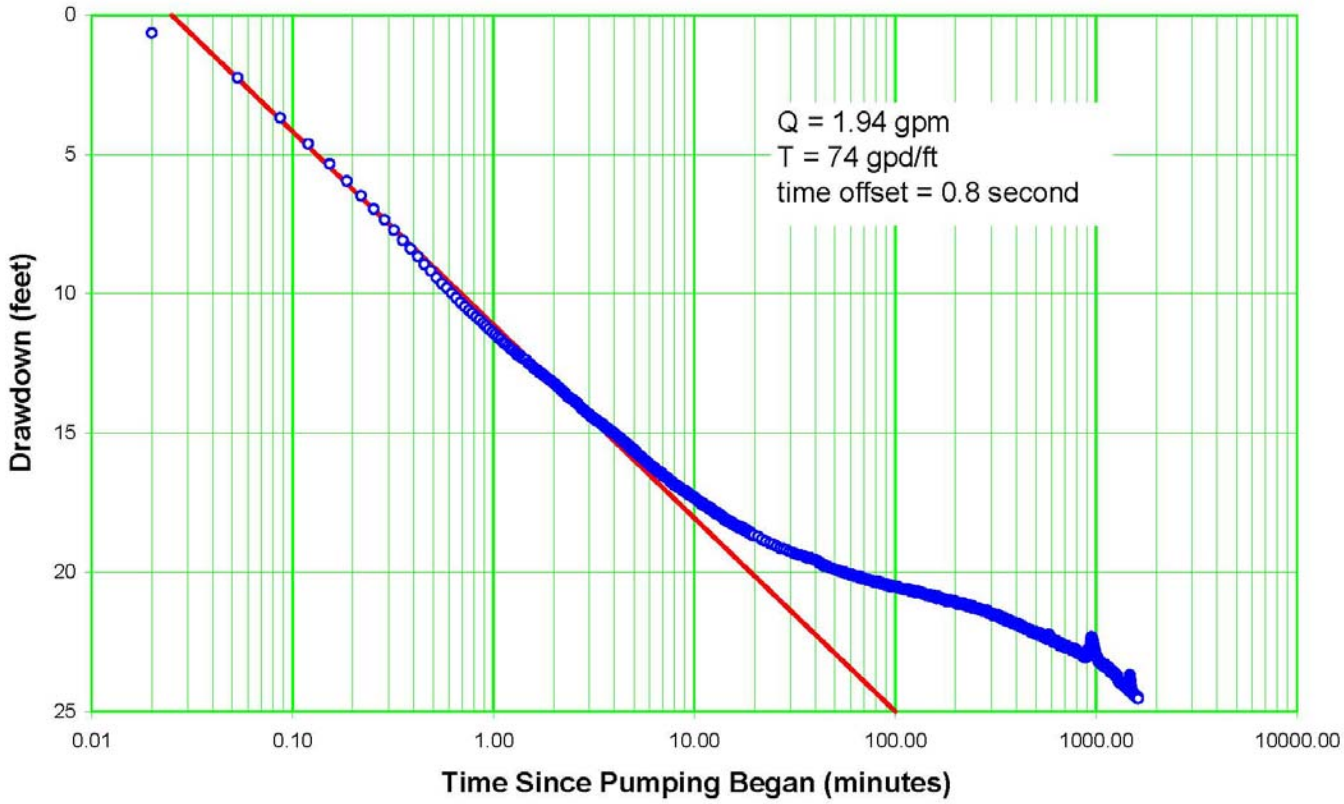

Figure 18. Well I-6 Drawdown - Theis Analysis

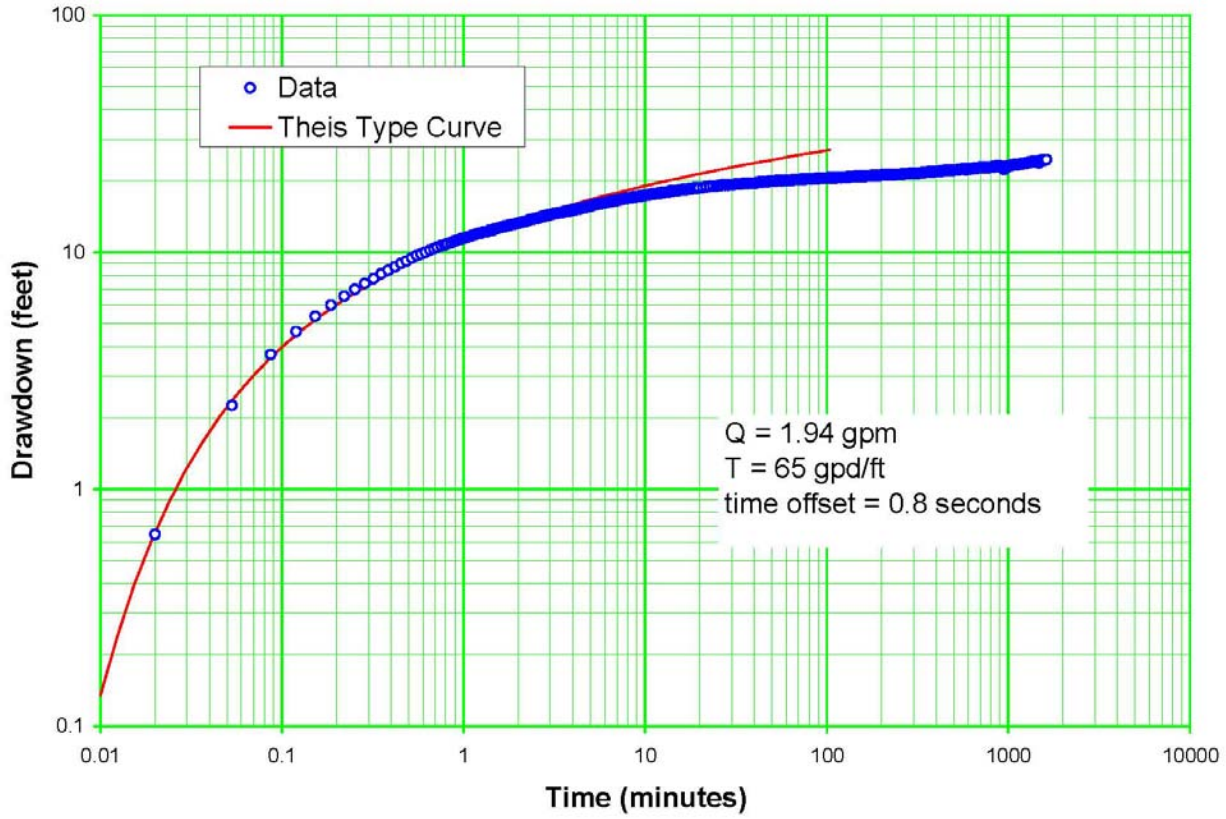

Figure 19. Well I-6 Drawdown - Late Data

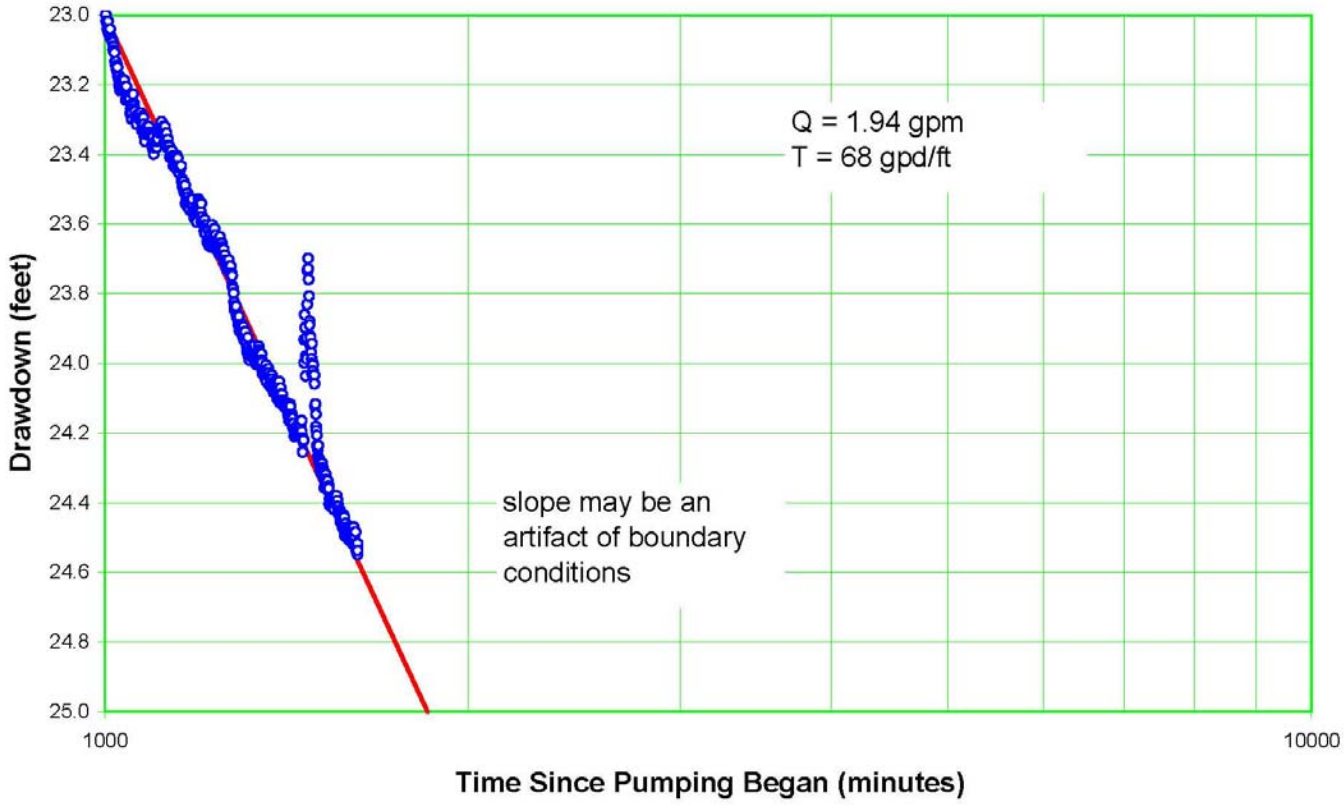

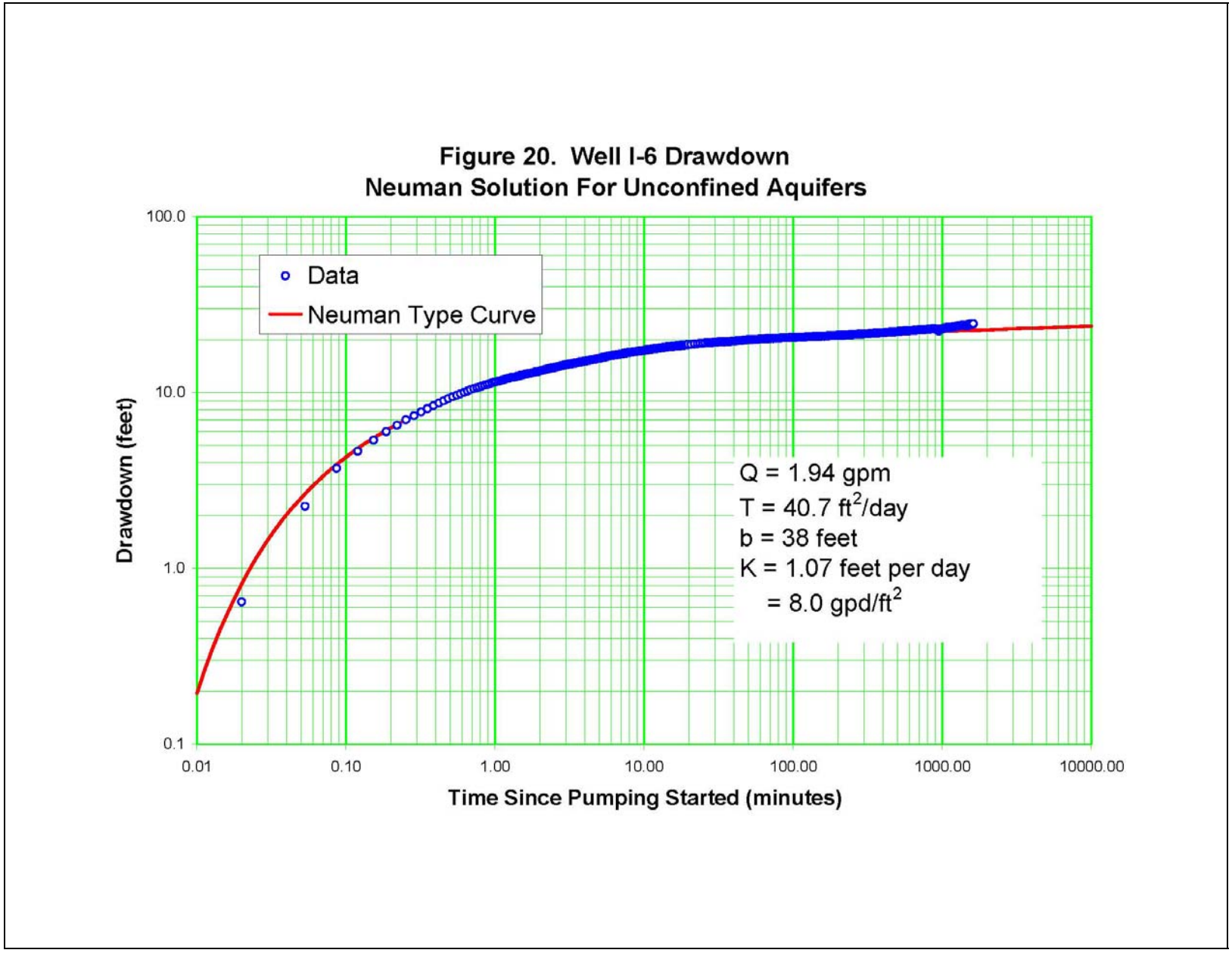
Figure 20. Well I-6 Drawdown
Neuman Solution For Unconfined Aquifers
Data
Neuman Type Curve
Q = 1.94 gpm
T = 40.7 ft2/day
b = 38 feet
K = 1.07 feet per day
= 8.0 gpd/ft2
Drawdown (feet)
100.0
10.0
1.0
0.1
0.01
0.10
1.00
10.00
100.00
1000.00
10000.00
Time Since Pumping Started (minutes)

Figure 21. Well I-6 Drawdown - Linear Plot

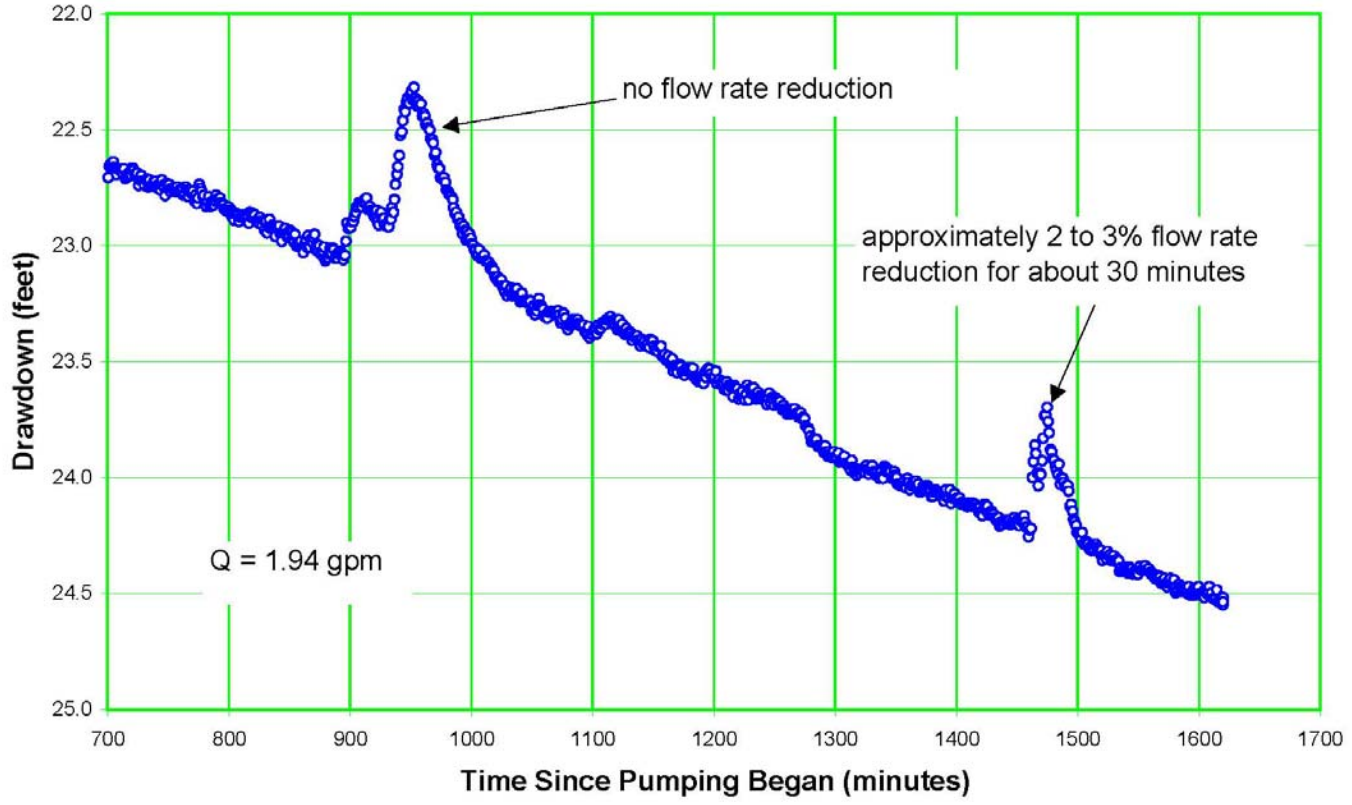

Figure 22. Well I-6 Recovery

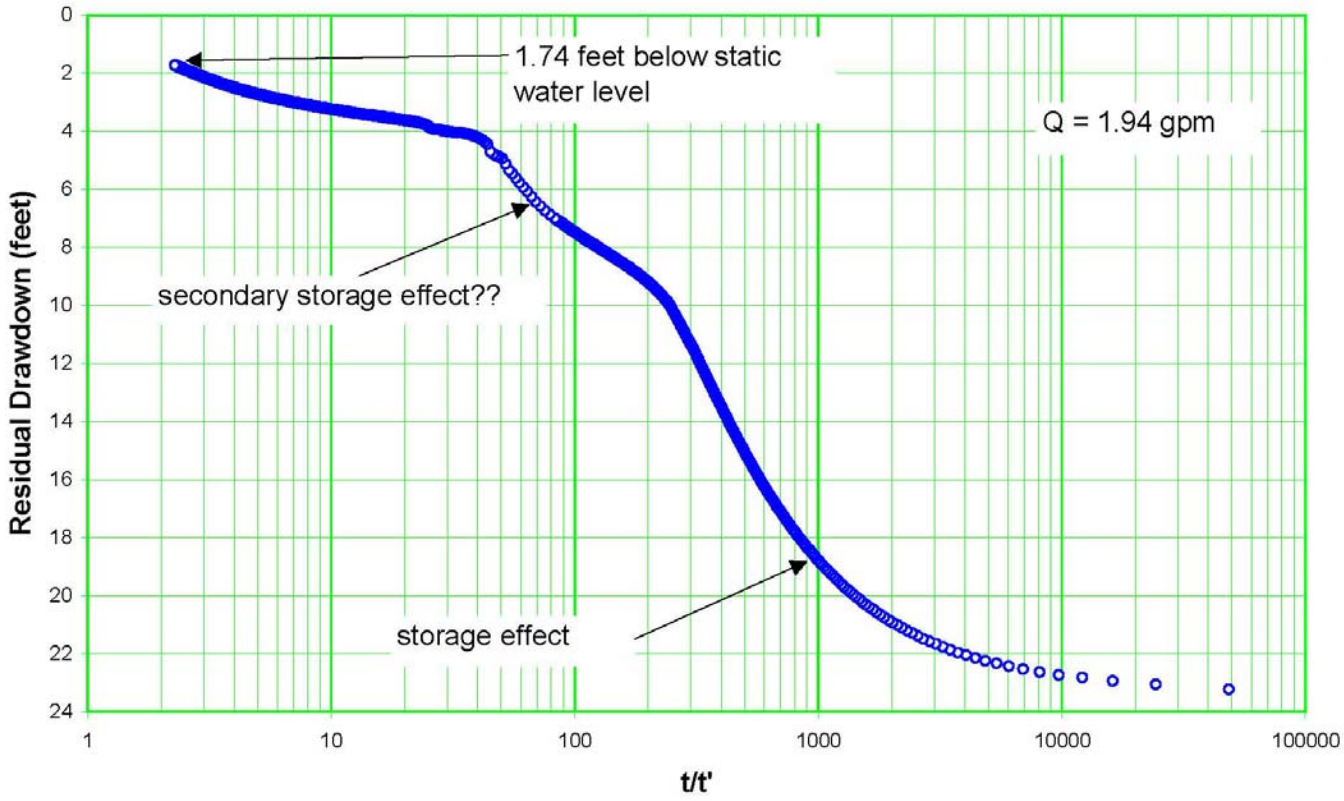

Figure 23. Comparison of Well I-6 Trial 3, Trial 4 and 27-Hour Test Recovery

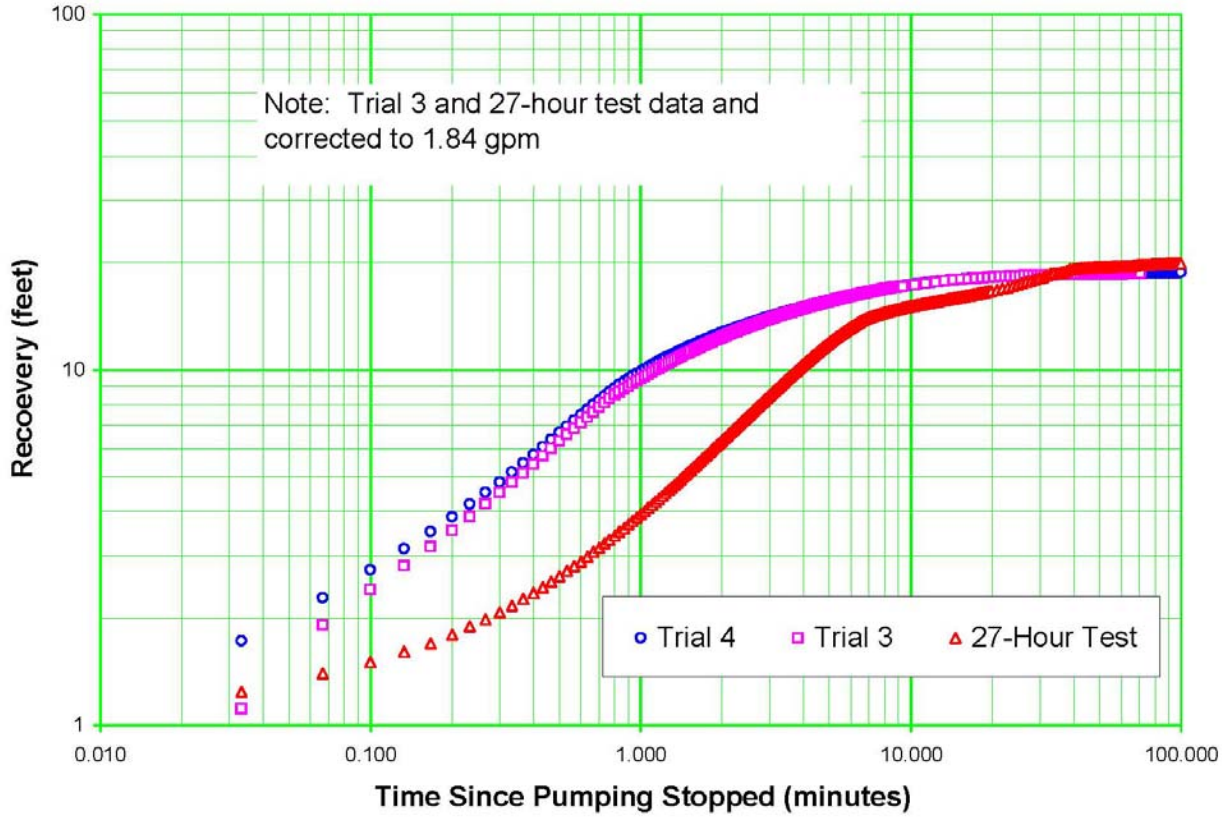

Figure 24. Well I-6 Comparison of Drawdown and Calculated Recovery

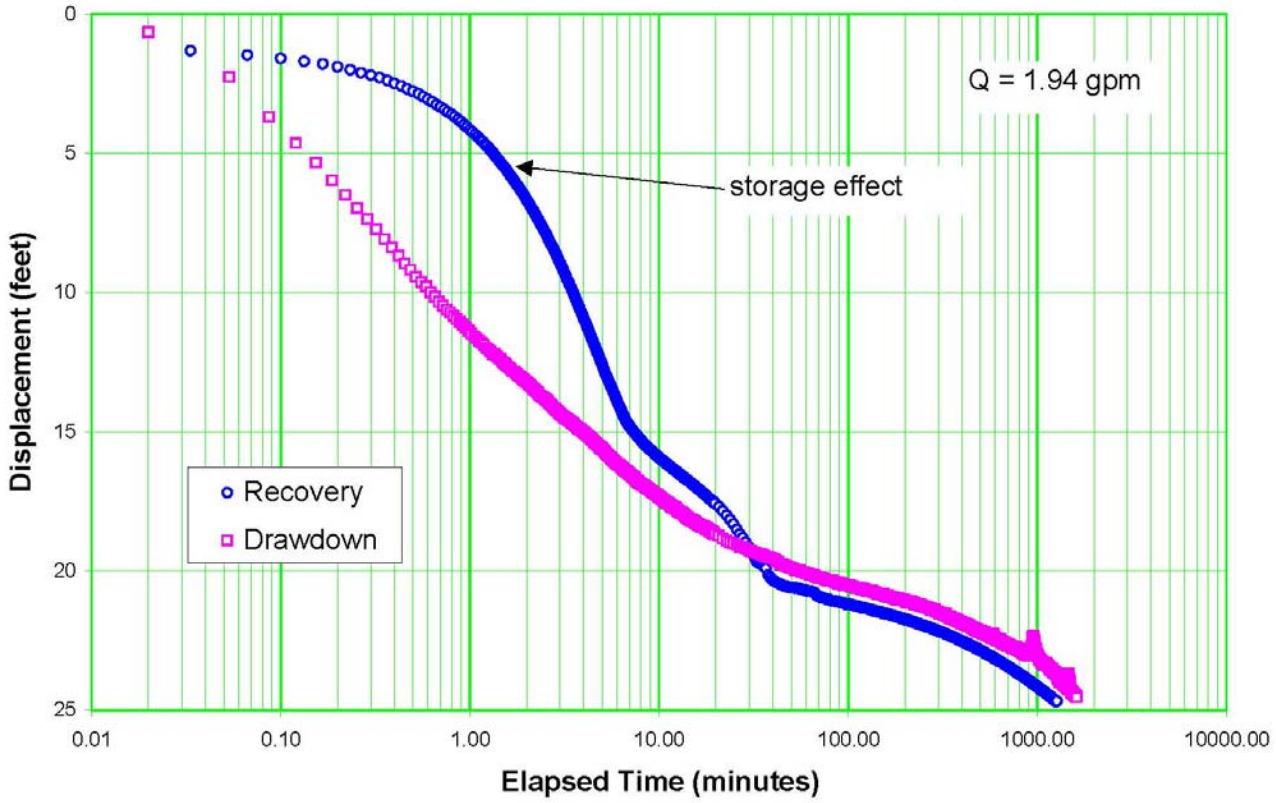

Figure 25. Packer Deflation Following Final Recovery

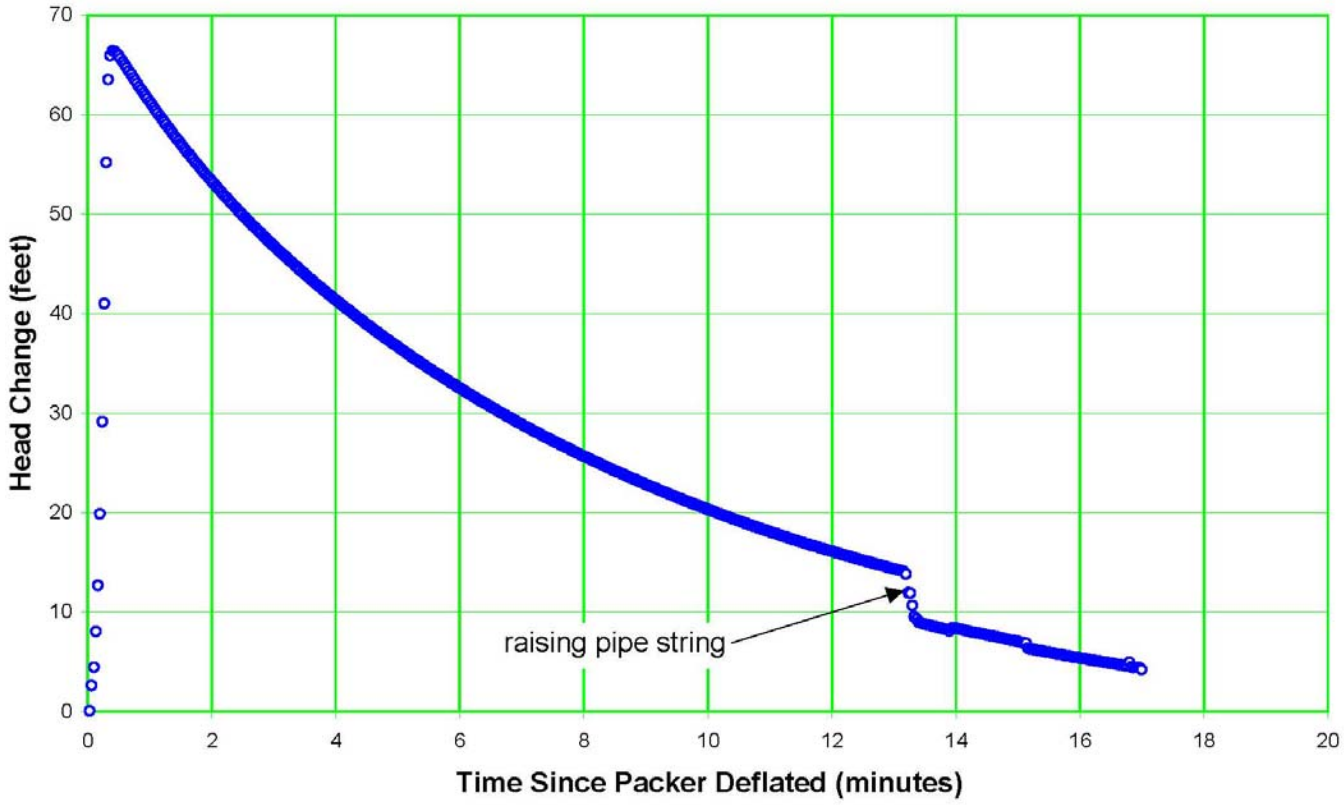

Figure 26. Packer Deflation Slug Test Analysis